Liver organ-on-chip models for toxicity studies and risk assessment

Taha Messelmani, Lisa Morisseau, Yasuyuki Sakai, Cécile Legallais, Anne Le Goff, Eric Leclerc, Rachid Jellali

Liver organ-on-chip models for toxicity studies and risk assessment

Taha Messelmani [1≠], Lisa Morisseau [1≠], Yasuyuki Sakai [2,3], Cécile Legallais [1], Anne Le Goff [1], Eric Leclerc [2*], Rachid Jellali [1*]

[1] *Université de technologie de Compiègne, CNRS, Biomechanics and Bioengineering, Centre de recherche Royallieu CS 60319, 60203 Compiègne Cedex*

[2] *CNRS IRL 2820; Laboratory for Integrated Micro Mechatronic Systems, Institute of Industrial Science, University of Tokyo; 4-6-1 Komaba; Meguro-ku; Tokyo, 153-8505, Japan*

[3] *Department of Chemical Engineering, Faculty of Engineering, University of Tokyo, 7-3-1 Hongo, Bunkyo-ku, Tokyo, Japan*

≠ Authors with equal contribution

*** Corresponding author:** Dr Rachid Jellali **(**rachid.jellali@utc.fr**),** Dr Eric Leclerc **(**eleclerc@iis.u-tokyo.ac.jp**)**

Abstract

The liver is a key organ that plays a pivotal role in metabolism and ensures a variety of functions in the body, including homeostasis, synthesis of essential components, nutrient storage, and detoxification. As the centre of metabolism for exogenous molecules, the liver is continuously exposed to a wide range of compounds, such as drugs, pesticides, and environmental pollutants. Most of these compounds can cause hepatotoxicity and lead to severe and irreversible liver damage. To study the effects of chemicals and drugs on the liver, most commonly, animal models or *in vitro* 2D cell cultures are used. However, data obtained from animal models lose their relevance when extrapolated to the human metabolic situation and pose ethical concerns, while 2D static cultures are poorly predictive of human *in vivo* metabolism and toxicity. As a result, there is a widespread need to develop relevant *in vitro* liver models for toxicology studies. In recent years, progress in tissue engineering, biomaterials, microfabrication, and cell biology has created opportunities for more relevant *in vitro* models for toxicology studies. Of these models, liver organ-on-chip (OoC) has shown promising results by reproducing the *in vivo* behaviour of the cell/organ or a group of organs, the controlled physiological micro-environment, and *in vivo* cellular metabolic responses. In this review, we discuss the development of liver organ-on-chip technology and its use in toxicity studies. First, we introduce the physiology of the liver and summarize the traditional experimental models for toxicity studies. We then present liver OoC technology, including the general concept, materials used, cell sources, and different approaches. We review the prominent liver OoC and multi-OoC integrating the liver for drug and chemical toxicity studies. Finally, we conclude with the future challenges and directions for developing or improving liver OoC models.

1 Physiology of the liver

The liver is subdivided into 2 parts, a left and a right lobe. It is connected to the portal vein and the hepatic artery, which ensure respectively 75% and 25% of the blood supply, and the hepatic veins, which provide drainage. In addition, the bile ducts ensure the evacuation of exocrine secretions toward the intestine. The liver is constituted of approximatively 1 million lobules which are its constitutional unit. These lobules, most of the time, are hexagonal in shape, at each corner of the hexagon is a portal triad which consists of a hepatic artery, a portal vein and a bile duct. The central vein on the other hand crosses the centre of the lobular structure (Fig. 1) [1]. The hepatic acinus is considered the functional unit of the liver and defined by the surface between two neighbouring central veins and two neighbouring portal triads (overlapping between two lobules, Fig. 1) [2,3]. The liver is composed of at least 15 different types of cell. Hepatocytes (parenchymal cells) represent approximatively 60% of the total cells and 80% of the total volume of the liver [4]. Followed by the non-parenchymal cells (NPC, 40% of the total cells): sinusoidal endothelial cells (LSECs, ~16%), Kupffer cells (15%), hepatic stellate cells (HSCs, 5%) and biliary epithelial cells [4].

The hepatocytes are polarized cells responsible of the major metabolic activities happening when an internal or external substance arrives to the liver. Their high metabolic activity is due to the large number of organelles each cell has. In addition, hepatocytes are the major cells involved in the metabolism of xenobiotics with the implication of the cytochrome P450 enzyme complex [5]. The LSEC are specialized endothelial cells forming the primary barrier between the blood and hepatocytes. These specialized endothelial cells are known to be the most permeable endothelial cells of the body due to the presence of fenestrae in their membrane and their high endocytosis capacity. The LSECs have vital physiological and immunological functions due to their exposition to the major changes happening in the liver during the digestion [6]. These functions include filtration of fluids and particles passing through the blood and the space of Disse, antigen presentation to the immune cells and initiation of liver regeneration following an acute liver injury [7]. LSECs are also directly implied in the

hepatocellular carcinoma development and its progression in addition to the initiation of inflammation. The inflammation is initiated after the presentation of the antigens by the LSEC to the local immune system of the liver also called Kupffer cells [7]. they are derived from monocytes and characterized by a high phagocytic potential. They produce cytokines that induce the inflammatory reaction and ensure the crosstalk between the other resident cells. Finally, the hepatic stellate cells also known as fat-storing cells is a major storage site for vitamins and lipids [8]. In addition, they produce the liver extracellular matrix which is composed of 5 to 10% of collagen in addition to glycoproteins, laminin, vitronectin, fibronectin and proteoglycans [9].

The liver is considered as a unique organ due to its irrigation by both arterial (hepatic artery, ~25%) and venous (portal circulation, ~ 75%) blood through the liver sinusoid (Fig. 1). This irrigation creates a temporal and zonal distribution of oxygen, nutrient and hormone concentrations in the various zones of the liver lobules [10,11]. The variation of these components, especially the oxygen tension, regulates the liver zonation and functionality. Indeed, the segregation of the liver into different zones creates different hepatocytes functions depending on their location in the different zones of the lobule. The zones can be divided following the oxygen and glucose gradient resulting in a high albumin and urea synthesis for the hepatocytes exposed to relatively rich oxygen and glucose at the periphery of the lobules and an increased glycolysis for the internal cells [5,12,13] (Fig. 1). The hepatotoxicity of exogenous molecules is also directly affected by the zonation phenomena. The zones with a rich oxygen tension correspond to the region where the CYP activity and the cells are less damaged and vice versa which leads to differences in hepatotoxicity. Such heterogeneity and specificity are considered as a survival strategy for each cell to perform simultaneously, independently and using the resources efficiently [4,12,13].

Fig. 1

1.1 Liver metabolic activity

More than 500 vital functions have been identified and associated with the liver. It plays an important role in glucose homeostasis by transforming excess circulating glucose into glycogen (glycogenesis), or by degrading stored glycogen into glucose (glycolysis). In the absence of glycogen, the liver synthesizes glucose from lactate, glycerol, or amino acids (gluconeogenesis) [14]. The liver is involved in the digestive system by secreting bile, a fluid produced by hepatocytes, secreted into bile ducts through bile canaliculi, and excreted into the duodenum. Bile emulsifies non-soluble compounds such as lipids, cholesterol and vitamins, and facilitates their absorption and digestion [15]. In addition to bile, the liver synthesizes many proteins and amino acids and plays a key role in lipid metabolism. Liver hepatocytes are the only cell type producing albumin, which is a carrier protein for hydrophobic substances such as hormones, vitamins, and enzymes. Albumin helps maintain the volume balance between blood plasma and interstitial fluid [16].

Another major role played by the liver is the storage and metabolism of fat-soluble vitamins. Vitamins are essential constituents that play an important role in catalyzing metabolic reactions to produce energy [17]. They are provided mainly by external contributions such as food as only a few are synthesized by the body, but they remain in insufficient quantity to allow its metabolic reactions to function properly. Most vitamins are not presented as a single specific molecule, but rather as a group of related compounds that provide the essential molecular ingredient. Many of these vitamins are concentrated, metabolized in active molecules, and stored in the liver, especially the fat-soluble vitamins [18]. They reach the liver through the intestines via absorption as chylomicrons or very low-density lipoproteins (VLDL). Of these vitamins, vitamin A is stored in stellate cells and can be oxidized to retinoic acid and then to retina for phototransduction. It can also be conjugated into glucuronide to be secreted in the bile. Vitamin D3 for its part, and regardless of its source, must undergo 25-hydroxylation by the CYP-450 system in the liver followed by hydroxylation in the kidneys for it to be functional [18].

1.2 Metabolism of xenobiotics

In addition to the numerous metabolic activities, the liver ensures the metabolism of xenobiotics. Xenobiotics are natural or synthetic substances which occur in the living organism, but which are foreign to it. They can come from drug use, auto-intoxication, or the chemical industry *via* environmental, food and water pollution. Such molecules can cause acute or subacute, chronic, or repeated toxicity, depending on the dose. Deactivating and eliminating xenobiotics usually takes place in the liver. By carrying out biotransformation, the liver's hepatocytes transform the xenobiotics, from being mainly lipophilic, to mainly hydrophilic, thus facilitating their elimination [2]. This is done by a succession of enzymatic reactions (oxidation, reduction, hydrolysis, etc.) via the enzymatic complex of cytochromes P450. Their metabolisms go through two reactions, Phase I and Phase II. Although most drug metabolism reactions in the liver aim to break xenobiotics down, for some drugs during the first hepatic passage, the pharmacologically inactive molecule may become active to overcome problems related to bioavailability and adsorption. The drug is introduced into the body in an inactive form and is activated by the liver, which we generally refer to as a prodrug [19].

Phase I metabolic reactions are characterized by enzymes from the cytochrome P450 superfamily (CYP450). These enzymes were discovered in the late 1980s and encompass more than 115 genes and pseudogenes. They are labelled with CYP1A1 up to CYP51P3 and are distributed in different proportions. By analyzing the total protein quantity of CYP450, we find mainly CYP3A4 at 22.1%, CYP2E1 at 15.3% and CYP2C9 at 14.6% [20]. CYP450 enzymes can be classified according to their substrates (xenobiotics, fatty acids, vitamins, eicosanoids, sterols, etc.). The main role of these enzymes is to modify the foreign substances (mainly lipophilic products) to facilitate their excretion by the liver and kidneys. They catalyse a series of reactions, mainly oxidation, by adding one or more oxygen atoms to the foreign substance. However, they can also catalyse other reactions, such as sulfoxidation, aromatic

hydroxylation, aliphatic hydroxylation, N-dealkylation, O-dealkylation and desamination [21]. The xenobiotics metabolized in phase I are conjugated enzymatically, in phase II, with a hydrophilic compound by a transferase enzyme such as glucuronyltransferase, sulfotransferase and glutathione S-transferase. These reactions aim to transform the molecules into soluble substances to facilitate their elimination through the bile and urine [22], although the phase I and II metabolic reactions mainly contribute to the elimination of the most pharmacologically-active compound. They can also bioactivate prodrugs into their active metabolite. These reactions promote the appearance of new substances (metabolized or bioactivated), and their accumulation in the liver causes a disruption in intracellular homeostasis, inducing toxicity or an idiosyncratic cascade leading to apoptosis or necrosis [22].

2 Current experimental liver models for toxicity studies

Considering the role of the liver in the metabolism of exogenous molecules, plus its exposure to a variety of potentially toxic compounds, it is important to use experimental models to anticipate hepatotoxicity. A successful model should sustain liver-specific function and accurately predict human *in vivo* responses to exogenous toxicants [23]. To perform toxicological studies and pharmacological tests, several experimental models are used in laboratories. They can be classified as *in vivo* (animal experimentation), *ex vivo*, and *in vitro* tests.

2.1 Animal experimentation

Animal models are of undeniable value in medical research, and murine models have been playing an essential role in studies on both xenobiotic toxicity and liver pathologies. Rodent models (mice, rats, and guinea pigs) are used in the first line to study hepatotoxic damage. The mechanisms of toxicity appear to be the same in rodents and humans for certain drugs, like acetaminophen (APAP). Mice remain the preferred model for APAP overdose studies due to the similarity in the toxic doses in both species [24]. Nonetheless, species-specific differences in characteristics between rodents and humans have become apparent as

research progresses. Thus, to bridge this gap, chimeric mice with livers repopulated by human hepatocytes have been developed. The livers of these chimeric mice express human drug-metabolizing enzymes, making it possible to better predict human disposition of drugs with a human-specific metabolism [25,26].

Current regulatory guidelines usually require safety and tolerability data from two species: a rodent and a non-rodent, before administering potential new medicines to humans in the first clinical trials [27,28]. Dogs are the default non-rodent used in toxicology studies with multiple scientific advantages, including similarity in the organs and physiology, adequate background data and availability [27,29]. Rabbits are mostly used to evaluate reproductive and developmental toxicity as they are phylogenetically close to humans [30]. Moreover, they are relevant models for safety and pharmacology studies as their cardiovascular system has structural similarities with that of humans [31]. Recently, minipigs have increasingly replaced dogs and rabbits in toxicology studies (particularly in the EU) due to ethical and scientific advantages. Minipigs effectively exhibit relevant similarity to humans: skin, cardiovascular system, gastrointestinal tract anatomy, and breeding habits [27,31].

Significant interspecies differences in metabolism exist that confound the direct extrapolation of data from laboratory animal species into man in the development of pharmaceuticals [27,32]. Non-Human Primates (NHPs), composed of monkeys and apes, are phylogenetically closer to humans than other species but involve high study costs associated with ethical issues [33]. Although animal models have significantly contributed to medical research, drug screening, and toxicity studies, they present two major disadvantages: significant interspecies differences with humans, and ethical considerations.

2.2 Human *ex vivo* models

Many commonly used *ex vivo* hepatotoxicity assays rely on liver slices, and whole perfused livers. Liver slices consist of maintaining the viability of all the cell types of the liver, as well as the multicellular histoarchitecture of the hepatic environment [34]. Human precision-cut liver slices (PCLS) are usually obtained from partial hepatectomies, surgical waste to be discarded,

explanted tissue, or non-transplantable tissue. Cell viability can be maintained for up to 5 days in standard cultures [35] and recent reports suggest that this may be extended to 15 to 21 days under precise conditions [36].

Preserving the complex cellular interactions, the original 3D architecture, and the lobular structure of the liver in human PCLS provide the essential requirement for a good model, increasing the investigation of xenobiotic toxicity and our understanding of the pathophysiology of different liver diseases. Despite many similarities, it is important to notice altered gene expression between liver slices and the liver. During PCLS culture, inflammatory genes are upregulated and, in contrast, genes involved in xenobiotics and lipid metabolism are significantly downregulated. This contrast in gene expression between *ex vivo* and *in vivo* conditions is mostly explained by the activation of several adaptation and stress responses to the new environmental condition of PCLS [35]. Another disadvantage of using PCLS in toxicology is the laborious preparation and culture procedure that may differ from operator to operator. Moreover, the short lifespan of PCLS can be an obstacle to studying the chronic effects of drug and chemical exposure. In addition, poor penetration of compounds into the inner cell layers of slices and inter-assay variability due to different preservation of cells in different slices have been reported [37,38]. On the other hand, it is important to specify that PCLS are mostly prepared from rat livers and are used in comparison and extrapolation to the human situation.

2.3 2D *in vitro* models

Today, due to the aim of replacing animal experiments whenever possible (3R), most liver hepatotoxicity studies rely on *in vitro* experimental models [39]. In the last 60 years, hepatocyte *in vitro* assays have focused on evaluating ADMET (Absorption, Distribution, Metabolism, Excretion and Toxicology) of new drugs using 2D cell cultures [40,41]. Thus, there are several *in vitro* liver models that differ depending on their culture conditions and conformations, cell types used and other additional culture parameters [42].

Primary hepatocyte suspensions are an easy method for performing high-throughput toxicity studies [43]. Some studies demonstrated that hepatocyte suspension provides a more accurate estimate of internal clearance rates and retains a higher level of functionality when compared to conventional monolayer culture [44–46]. However, isolation protocols and the lack of cell-matrix/cell-cell contact leads to a loss of cell polarity, integrity, and dedifferentiation. Thus, hepatocytes in suspension have a short life-span (often a few hours) which is insufficient for developing and studying toxicity [23].

Static monolayer culture is the conventional 2D cellular model [23,47]. Animal or human hepatocytes are grown in plastic Petri dishes and are exposed to changes in nutrient concentrations and catabolite accumulation over time. Periodically refreshing culture medium is necessary to remove accumulated catabolites and renew nutrients. Under standard culture conditions, hepatocytes can preserve cell-cell interactions and liver specific function, making possible a wide range of applications: short-term hepatotoxicity, cytochrome P450 induction and inhibition, drug interactions, pharmacokinetics, and pharmaco-dynamics. Furthermore, this 2D cellular model system is easier to manipulate in the laboratory, is low cost, and is much more widely accepted ethically than the use of animal models [48,49]. Although 2D cell culture models basically have some advantages, they are limited in their applications. Current mainstream 2D models fail either to capture the complexities of multicellularity or to maintain cell phenotypic characteristics for long cultivation. On the other hand, when using animal cells similar to *in vivo* animal experiments, it is difficult to obtain an accurate *in vitro-in vivo* extrapolation in humans using *in vitro* models based on animal cells [50].

Sandwich-cultured hepatocytes (SCH) are a powerful *in vitro* tool that can be used to study hepatobiliary drug transport, species differences in drug transport, transport protein regulation, drug-drug interactions, and hepatotoxicity [47]. This model is composed of primary hepatocytes cultured between two layers of extracellular matrix, traditionally collagen type I or Matrigel®. Maintaining hepatocytes in a sandwich-cultured configuration increases and maintains albumin secretion, cell morphology and polarized architecture, cell viability, basal and induced enzyme activities, and mimics *in vivo* biliary excretion rates [23,48–50]. For these reasons,

sandwich-cultured hepatocytes are a pertinent *in vitro* model for investigating drug-drug interactions, clearance predictions and the mechanisms underlying hepatotoxicity, such as cholestasis [51–54]. Despite the great potential attributed to this culture technique, expression of the genes responsible for the detoxification function of the liver decreases over time due to cell dedifferentiation. However, gene expression of phase II enzymes remains at a relatively high level in comparison with monolayer hepatocyte culture [23,55–57]. Another limitation of the sandwich-cultured hepatocytes model is the batch-to-batch variation in extracellular matrix substrates. Therefore, several approaches to overcome the limitations of the *in vitro* liver models have been proposed, including adjusting components of the culture medium and extracellular matrix, changing the cell culture format from monolayer to 3D organization, adding flow to the culture system, and culturing hepatocytes with non-parenchymal cells.

2.4 3D *in vitro* models

In recent decades, there has been much evidence indicating that 3D cell culture more accurately reflects *in vivo* physiology by mimicking the architecture and cell-cell contacts found in intact tissue [58]. Thus, more and more research has focused on developing and optimizing various liver 3D culture strategies as superior tools for a multitude of applications in drug development [59].

One strategy for 3D hepatic tissues is to cultivate cells within scaffolds. These scaffolds are composed of natural or synthetic materials such as alginate, Matrigel®, loofa sponge or poly(lactic-co-glycolic) acid (PLGA), and allowed to mimic *in vivo* conditions thanks to their macroporous (>100µm) structure and native representation of ECM, as well as their capacity to transport nutrients and waste during cell cultivation [60–63]. Furthermore, the specific functions of hepatocytes, such as albumin synthesis, urea secretion, and CYP activity, are sustained [64,65]. Despite the advantages of scaffold-based culture, problems with controlling pore size and porosity, large batch-to-batch variations upon isolation from biological tissues and poor biomechanical strength have been observed [60,66].

Hepatic spheroids were constructed, with the assumption that cellular aggregates better mimic liver tissue characteristics. These spheroids can be generated from primary hepatocytes, cell lines or stem cell-derived hepatocyte-like cells by using different methods, such as hanging drop or culture plastic dishes with a non-adhesive surface. Establishing 3D cell-cell contacts and the secretion of ECM proteins within hepatic spheroids ensures the maintenance of differentiated liver functions such as albumin production and metabolic activity [42,67]. Moreover, liver spheroids have been shown to be viable, functional, and stable in extended cultures of up to 4 to 5 weeks, unlike conventional hepatocyte 2D cultures (dedifferentiation after 2-3 days) [68]. Nevertheless, hepatic spheroids have limited applications because of the presence of a hypoxic/necrotic core within the spheroid due to low oxygen diffusion or accumulated bile acids [69,70]. Hepatic spheroids can also be encapsulated inside semi-permeable beads composed of biomaterials, such as alginate, and packed into a column to be perfused [71,72]. These systems preserve cell viability and functionality, as well as protecting cells from shear stress. Disadvantages include poor stability of the hepatocyte suspension, mass transfer problems, degradation of the microcapsules over time, and difficulties for cell retrieval [65,70].

Progress in 3D bioprinting technology has led to the development of 3D liver bioprinting technology. This culture system consists in the fabrication of complex 3D biomimetic architectures using precise layer-by-layer deposits of biological materials with spatial control thanks to a computer [73]. The three major bioprinting techniques are inkjet, laser-assisted, and extrusion bioprinting. Biological materials, called bio-inks, are composed of synthetic or natural hydrogel pre-polymer solution with encapsulated cells [74]. More recently, decellularized extracellular matrices have been used as bio-ink allowing the retention of a composition and relevant cues for cells [75]. Cells within 3D liver printing are in close proximity to each other, and rapidly form tight junctions and deposit their own ECM, yielding solid microtissues that resemble native liver in cellular density. This cell organization led to an increase in liver-specific gene expression, metabolic product secretion and CYP450 induction [60,76]. Furthermore, 3D liver printing has advantages in terms of precise control, repeatability,

scalability, and individual design. Nevertheless, printing techniques may reduce cell viability or induce other unknown consequences [74].

3 Liver organ-on-chip

As described above, several approaches have been developed in recent years to build an appropriate physiological micro-environment for liver tissue maintenance, and to improve the metabolic function of hepatocytes *in vitro*, including 3D cultures on scaffolds/hydrogels, spheroids, organoids and co-culture models [77,78]. These approaches improve liver tissue organization, cell-cell and cell-ECM interactions, cell polarization, and maintenance of the liver functions [78]. Nevertheless, despite their considerable advantages over traditional 2D culture models in Petri dishes, static 3D cultures still lack several key features essential for reproducing a physiologically relevant environment for liver cells. This is due to the absence of flow which is a key feature for the reproduction of mechanical cues (shear stress), zonation and multiple cell/organ co-cultures [79,80]. The integration of dynamic culture presents several advantages regarding to the cell's metabolism via the constant renewal of the culture medium by supplying nutrients and the evacuating the cumulative toxins. In addition, the multi-organ coupling associated with biological barriers allow a better understanding of the ADMET profile of newly discovered molecules [81]. In the last decade, organ-on-chip (OoC) technology has emerged as a promising alternative for overcoming these limitations by reproducing a more physiological microenvironment that reproduces the key biological features of cells and organs *in vivo* [79,80]. Thus, OoC technology appears to be a powerful tool for replacing the traditional paradigms based on animal experiments and 2D/3D *in vitro* static cell culture methods [82]. Fig. 2 illustrate and compare liver OoC technology with the different experimental liver model for toxicity studies.

Fig. 2

3.1 OoC technology

OoC technology refers to a class of microfluidic devices that make possible the culture of cells or tissues in a dynamic environment engineered to reproduce the physiological architecture and function, and the associated *in vivo* microenvironment [83]. These devices that mimic the functions of organs *in vitro* are also called microphysiological systems (MPS) [84]. An OoC consists of three principal elements: i) a microfluidic device, most commonly based on glass or polymeric material, with microchannels for medium perfusion and microchambers for cell culture; ii) living cells or tissues; iii) microfluidic flow (generated by a pump or pressure controller) through the device's inlet/outlet providing culture medium for the cells/tissues [85]. The cell culture in microfluidic biochips allows precise control of the cell micro-environment and can faithfully emulate multiple characteristics of native cells/organs: 3D architectures, cell-cell and cell-ECM interactions, continuous nutrient exchange and waste removing, zonation, physiological shear stress, and chemical gradients [80,83,86]. Using microfluidic devices can also efficiently reproduce physiological multiorgan interactions, where the multiple organ models cultured in separate biochips or multi-OoC platform are connected together through microfluidic tubing or microchannels [87–89]. Moreover, microfluidic technology offers the advantages of incorporating biosensors and bio-actuators to control the cultures, provide rapid analysis, and apply electrical or mechanical stimuli [85,86,88].

Selecting appropriate materials for the microfluidic device is one of the fundamental steps in OoC development. As the devices are used for biological applications and cultures of living cells, there are several parameters to consider regarding the choice of the material: biocompatibility, optical transparency for microscopic imaging, robust and tunable mechanical properties, ease of sterilization, chemical inertness and gas permeability [88,90,91]. The cost and ease of fabrication are also important factors when considering large-scale production and OoC standardization [90,91]. Due to its distinctive properties, including biocompatibility, good transparency, and permeability to oxygen, polydimethylsiloxane (PDMS) remains the most frequently used materiel for OoC devices [89,91,92]. In addition, PDMS is inexpensive, easily

processable with soft lithography for prototyping, and its elasticity makes it possible to replicate complex 3D microstructures with regular and precise patterns [92,93]. Nevertheless, PDMS also has several limitations, particularly strong absorption of hydrophobic molecules and incompatibility with mass production [91,94]. To overcome the drawbacks associated with PDMS-based OoC, glass can be used due to its outstanding properties, especially low drug absorptivity, transparency, and biocompatibility. However, glass remains costly and not gas permeable (suitable for cell culture) [91,95]. In the last decade, several alternative materials have been used for OoC applications. These alternatives include mainly elastomers and thermoplastic polymers: thermoset polyester (TPE), polyurethane (PU), styrene-(ethylene/butylene)-styrene (SEBS) copolymer, tetrafluoroethylene-propylene (FEPM), perfluoropolyether (PFPE), poly (methyl methacrylate) (PMMA), cyclic olefin copolymer (COC), polycarbonate (PC), polystyrene (PS), poly (vinyl chloride) (PVC), polysulfone, poly (lactic acid) and polytetrafluoroethylene (PTFE) [91,95–99]. Of the polymeric materials, thermoplastics are excellent candidates for large-scale production and commercialization as they are low-cost and can be processed by injection molding [97]. Combining two or more materials is another promising approach for developing hybrid devices drawing benefits from different substrates while avoiding their limitations. In recent years, several hybrid microfluidic devices combining PDMS with PC, glass and COC or fluorinated ethylene propylene (FEP) with COC have been reported in the literature [100–103]. Recently, progress in 3D printing has offered the opportunity to introduce new materials, such as hydrogels (naturel or synthetic): collagen, alginate, gelatine, hyaluronic acid, polyethylene glycol (PEG), polylactic acid (PLA), polylactic-co-glycolic acid (PLGA) and polycaprolactone (PCL) [91,104,105].

Microfluidic devices can be manufactured using various microfabrication methods, including photolithography, soft lithography, laser and chemical etching, micromilling, hot embossing, injection moulding and 3D printing [90,106]. The choice of manufacturing process depends on the material. As PDMS is the preferred OoC substrate, soft lithography or replica moulding remains the most common microfabrication technique for OoC [106]. Soft lithography implies the casting of a mixture of liquid PDMS and a curing agent on a mould previously

manufactured by lithography or etching. After curing by heating, the micro-structured PDMS layer is peeled from the mould and sealed to a glass cover or another PDMS layer using plasma treatment to form the microfluidic device [83,107]. Hot embossing and injection moulding, two processes suitable for industrial production, are the methods of choice to process thermoplastics [97,107]. In both processes, molten materials (under high pressure and temperatures) are brought into contact with the mould and the patterned device is obtained after cooling [107,108]. The bonding of such thermoplastic devices can be achieved using thermal fusion, solvents, surface modification and adhesives [107]. Of the new technologies, 3D printing has emerged in recent years as a promising tool for microfluidic biochip manufacturing. 3D printing, or additive manufacturing, is a process of creating layer-by-layer a 3D object through the selective application of materials [104,108]. There are three main 3D printing techniques suitable for microfluidic biochip manufacturing: stereolithography (SL), fused deposition modelling (FDM) and photopolymer jetting (multi-jet modelling, MJM) [104,106,109]. The use of 3D printing offers several advantages, including the rapid and cost-effective production of devices with highly complex architectures and shapes, and the possibility of easily integrating various elements into the microfluidic device, such as sensors, connectors and valves [109–111]. The major limitation of 3D printing technology is the insufficient patterning resolution and the non-transparency of the materials, which excludes microscopic imaging (necessary in microfluidic applications) [89,104].

3.2 Cell sources for liver OoC

In addition to the microfluidic biochip design and material, the choice of cell types and sources is crucial for building correct and physiologically relevant *in vitro* liver OoC models. Hepatocytes represent approximately 60% of the total liver cells and are responsible for most hepatic functions. Thus, hepatocytes are the major/unique cell type in a liver OoC. The potential hepatocyte sources for liver OoC can be divided into three main groups: primary cells (animal and human), immortalized cells, and induced pluripotent stem cells (iPSCs) [10,80]. The advantages and limitations of the different types of hepatocyte are presented in Fig. 3. To

construct liver OoC models that adequately reflect the complexity and functionalities of the liver, hepatocytes can be cultured with non-parenchymal cells (NPCs): liver sinusoidal endothelial cells (LSECs), Kupffer cells (KCs), hepatic stellate cells (HSCs) and cholangiocytes.

Fig. 3

3.2.1 Primary hepatocytes

Primary human hepatocytes (PHH) obtained from liver biopsies or non-transplantable livers are still considered to be the gold standard for developing human-relevant *in vitro* liver models. Due to their origin, they accurately reflect the physiology and functionality of the liver and represent an invaluable model for *in vitro* drug metabolism and toxicity studies [10,112,113]. Moreover, the development of cryopreservation protocols has facilitated access to PHHs and their use for *in vitro* models [112,114]. PHHs lose their phenotypes and functionalities after two/three days when cultured in a 2D static environment [115]. Nowadays, progress in tissue engineering and microfabrication (3D spheroids and hydroscaffold culture, and OoC) makes it possible to maintain functional PHH cultures for several weeks [69,80,112,116,117]. However, despite the progress in hepatocyte extraction, cryopreservation and culture, the use of PHHs remains limited by several factors, including the inability to proliferate, high costs, limited availability, and batch-to-batch variability [112,113].

Primary hepatocytes from animals can be also used for *in vitro* liver models. These hepatocytes, especially from rats and mice, are widely used because of their attractivity. They represent an abundant source of fresh primary cells and exhibit good stability and hepatic functionality in culture [10]. However, there are considerable limitations for the use of animal hepatocytes: functional differences between animal and human hepatocytes (differential cytochrome activity), inter-species variability and ethical concerns [10,114,118]. In recent years, the use of Upcyte hepatocytes for drug metabolism and toxicity studies has been reported in several works [119–121]. Upcyte hepatocytes are PHHs genetically modified to acquire

proliferative capacity without being immortalized and retaining the phenotype of primary cells [119]. Nevertheless, although these cells present several interesting properties, there is a considerable lack of information regarding their phenotypic stability and performance (compared to other cell sources) [70].

3.2.2 Hepatic cell lines

The alternative choices to PHHs are immortalized hepatic cell lines, such as HepaRG, Fa2N-4, HepG2/C3A, Hep3B, Huh7 [122]. Cell lines are derived from tumour tissue (hepatocellular carcinoma) or generated by immortalization of primary hepatocytes [122]. These cells are widely used in drug metabolism and toxicology studies due to their many advantages, including the unlimited propagation potential, ease of use, good availability, stable phenotype, lack of inter-donor variability, and low costs [112,123]. However, they present limited performances and functionalities regarding metabolic activity and sensitivity to hepatotoxins and are only suitable for the early stages of drug or chemical evaluations [10,124,125]. Among immortalized cells, the human hepatocellular carcinoma-derived HepG2/C3A line is one of the most commonly used for *in vitro* liver models [126]. Although HepG2/C3A exhibit several hepatic characteristics (albumin secretion, metabolism of several xenobiotics), they lack relevance for drug screening and toxicity studies because of their low and variable levels of CYP450 enzymatic activity and poor expression of transporters [80,114,126]. HepaRG cells, human bipotent progenitor cells, are an interesting alternative to PHHs for preclinical drug metabolism and hepatotoxicity assessments. Altogether, HepaRG present similar features to those of PHHs, including high expression of phase I and II drug metabolizing enzymes, secretion of liver plasma proteins and of hepatobiliary transporters [112,127]. The major drawbacks of these cells are the use of DMSO for differentiation, and the long culture process.

3.2.3 Human induced pluripotent stem cells (hiPSCs)

In recent decades, human hepatocyte-like cells (HLCs) derived from stem cells (adult stem cells and pluripotent stem cells PSCs) have emerged as an attractive cell source for *in vitro* liver models, with the potential for large-scale production. Stem cells are capable of self-renewing and differentiating into mature cells of a particular tissue type, allowing the generation of all cell types from the human body [112,128]. Of these stem cells, PSCs, i.e. embryonic stem cells (ESCs) and induced pluripotent stem cells (iPSCs), are the most commonly studied for differentiation in HLCs [129]. The use of human embryonic stem cells (hESCs) raises ethical problems and is strictly regulated, or even prohibited in many countries [130]. iPSCs can be obtained from somatic cells following the reprogramming technology developed by Yamanaka's team [131]. Contrary to ESCs, hiPSCs raise fewer ethical problems and can be easily established from abundant cell sources such as skin fibroblasts, blood cells, and renal epithelial cells in urine samples [132]. Currently, it is assumed that hiPSCs can be differentiated using several protocols and generate HLCs reproducing many hepatic features, including morphology, albumin and urea secretion, glycogen storage, and drug metabolism [10,112,133,134]. In addition to availability, the advantages of hiPSCs include minor batch variability and good sensitivity (comparable to PHHs) for detecting drugs causing hepatotoxicity [126,135]. Therefore, hiPSCs could provide a limitless supply of hepatocytes for drug/chemical hepatotoxicity assessments. However, there are still some limitations to the widespread use of hiPSCs: incomplete maturation of hepatocytes, epigenetic memory, and high cost and experimentation time [10].

3.2.4 Non-parenchymal cells (NPCs)

As for PHHs, there are three main sources of NPCs for liver OoC development: primary cells, hepatic cell lines, and hiPSCs [10,136]. Human primary LSECs, KCs and HSCs can be isolated, separately or simultaneously, from the liver using the same protocol as hepatocytes (enzymatic digestion) [112]. Although primary NPCs are the best choice for reproducing the *in vivo* microenvironment, their use is limited due to scarce availability, low yield and the

presence of impurities during the isolation process, high costs and rapid loss of functions in *in vitro* culture (such as loss of fenestration for LSECs and non-specific activation for HSCs and KCs) [10,137,138]. As an alternative to primary NPCs, several immortalized cell lines have been developed and used in co-culture with hepatocytes: TMNK-1, TRP3 and SKHEP-1 for LSECs; hTERT-HSC, GREF-X, LI90, TWNT-1, LX-1 and LX-2 for HSCs; THP-1 and U-937 for KCs, and MMNK and HepaRG for cholangiocytes [10,136–139]. However, immortalized NPCs lack the main features of primary cells and do not emulate *in vivo* physiology [10,136]. In recent years, several protocols have been proposed for iPSC differentiation into LSECs [140,141], HSCs [128,140,142], KCs [143] and cholangiocytes [144,145]. Nevertheless, contrary to the abundance of studies related to HLC generation, only a few protocols have aimed to differentiate iPSCs into NPCs. Moreover, the cells obtained are only partially mature and the protocols used still need to be improved by optimizing culture medium (small molecules and growth factors concentrations), supports of culture (3D, ECM and dynamic microfluidic cultures) and coculture of different liver cell types [146].

3.3 Different liver OoC approaches

3.3.1 2D monolayer culture

The most common approach when developing microfluidic systems for the monolayer culture of cells is based on lithography patterned substrates. It has been proven that culturing hepatocytes on these substrates enhances the hepatic functionalities by precisely and reproducibly controlling the distribution of the different cell types and providing biochemical cues for both parenchymal and non-parenchymal cells [147]. The pioneers of the liver-on-chip models were Allen & Bhatia, who developed a polysulfone-based perfusable flat-plate bioreactor and used it to co-culture primary rat hepatocytes with fibroblasts from the cell line J2-3T3 [148,149]. Comparing their developed model with conventional static 6-well plates, they demonstrated that the oxygen gradients produced by the flow circulation recreated regional compartmentalization, which mimics the liver zonation which cannot be observed in static plates.

Depending on the applications and the cell's preferences, different substrates and coatings can be used to enhance adhesion and proliferation. Jellali et al. proved that, depending on the substrates (PFPE or PDMS) and the coatings (fibronectin or collagen), the behaviour of the cells differed [98]. Schoenenberger et al. reported similar findings, demonstrating that cell (Madin-Darby canine kidney cell line, MDCK) adherence to fibronectin-coated surfaces was less effective than other proteins, such as collagen IV, collagen I, laminin and vitronectin [150]. To investigate the potential of liver biochips compared to conventional Petri dishes, Jellali et al. developed a microfluidic bioreactor for human hepatocyte culture [117]. The biochip was composed of microchambers connected by microchannels, allowing the circulation of culture medium inside the network, and was coated with collagen for hepatocyte adhesion. The hepatocytes retained their activity while showing increased expression of major cytochrome P450 genes and higher urea and albumin production in comparison with Petri dishes. In addition, when exposed to midazolam and phenacetin, the hepatocytes maintained their metabolic activity. This was confirmed by measuring CY3A4 and CYP1A2 activity which was 5000 and 100 times higher, respectively, in biochips than in Petri dishes. The authors successfully maintained the culture of functional hepatocytes in biochips for 13 days [117].

In the natural liver, hepatocytes are shielded by a layer of sinusoidal endothelial cells, which protects them from the direct shear of blood flow and influences mass transport consistency [151]. Xia et al. developed a laminar-flow perfusion bioreactor for immediate-overlay sandwich culture of hepatocytes. The bioreactor consists of an acrylic body and top sealed with an O-ring (Fig. 4A). First, the hepatocytes are extracted and seeded on a collagen-coated membrane and overlaid with collagen-coated inserts. Then, the system is secured with the O-rings. The sandwich cassette is then deposed in the cellular compartment of the bioreactor. The culture chamber is connected by two channels linked to a peristaltic pump for flow circulation. They successfully maintained liver specific functions for two weeks, with hepatocytes exhibiting restored polarity and biliary excretion. In addition, the cells produced sensitive and consistent drug toxicity responses [152].

3.3.2 Matrix-free liver spheroids/organoids-on-chip

The previously described two-dimensional (2D) monolayer culture does not reflect *in vivo* physiology where the tissues are in 3D with different topographical organization that affects cell responses [153]. Different approaches have been used to construct such a 3D communication network, like hanging drop, spinner flask, cells cultured on non-adherent surfaces, and micromoulding [154]. The principle of these methods consists of reassembling the cells by applying an external force or by conditioning the cells to self-assemble. The cells re-created in suspension pass through an aggregation step, followed by a compaction phenomenon to form compact 3D structures (spheroids or organoids). Weng et al. worked on developing a scaffold-free liver-on-chip mimicking the liver lobule [155]. This was achieved by cultivating primary hepatocytes and hepatic stellate cells (HSCs) on a micropatterned PDMS biochip. To obtain the 3D structure, the cells were deposited on the multi-layered collagen coated PDMS to form the 3D biological template. The system was enclosed with a hydrophilic flow diverter making possible vertical cell anchorage and connected to a peristaltic pump circulating the culture medium. The system was designed in a hexagonal form with six inlets and one central outlet mimicking the flow arriving from the portal vein and evacuated from the central vein. Following the flow diversion, the F-actin polarized to the peripheral cortex of the cells and developed a 3D intracellular skeletal network which formed a hierarchical tissue. Building the hepatic hierarchical organization mimicking *in vivo* conditions demonstrated the potential of the model in recreating hepatic zonation, which is a key feature for predicting hepatotoxicity.

Another approach is commonly used to form scaffold-free spheroids by cultivating cells in concave microwells. Ma et al. developed a concave microwell based on PDMS-membrane-PDMS sandwich multilayer chips for hepatocyte culture (Fig. 4B) [154]. The system integrated the possibility of forming scaffold-free spheroids using a V-shape structure and the mimicking of hepatic sinusoidal endothelial cells. The cells are seeded in PDMS V-shaped microwells for spheroid formation, then a perfusion system is mounted using a transwell-based microporous

membrane on top of which the culture medium circulates. This model demonstrated high cell viability and maintenance of hepatic polarity, liver-specific functions and improved metabolic activity compared to conventional perfusion methods.

Fig. 4

3.3.3 Scaffold/hydrogel-based 3D liver OoC

One of the main focuses of liver research and development is the 3D organization of cells to obtain relevant liver phenotypes and functionalities. In addition to the cell self-assembly methods cited above, 3D organization of cells can be obtained using a hydrogel/scaffold matrix (alginate, hyaluronic acid, gelatine, collagen, Matrigel) integrated within the biochip [125]. Using hydrogel and scaffold reproduces ECM behaviour and offers the possibility of tuning the cells' micro-environment by modifying the composition of the matrix and/or the mechanical properties [156,157]. Toh et al. developed a 3D hepatocyte chip (3D HepaTox Chip) based on a multiplex microfluidic channel allowing the 3D culture and maintenance of hepatocyte functions [158]. The biochip consists of a central culture compartment where cell suspension of hepatocytes is loaded using a single inlet. The cells were cultured in a methylated collagen and negatively-charged HEMA-MMA-MAA terpolymer, which is a matrix favouring the 3D organization of hepatocytes. The central chamber is flanked by 2 side perfusion compartments with elliptical micropillars through which the culture medium and drug solution pass by diffusion to the hepatocytes, generating a gradient of concentration. The hepatocytes cultured in the biochip showed cell-cell and cell-ECM interactions, maintained their metabolic functions, and made it possible to assess the hepatotoxicity of 5 model drugs (acetaminophen, diclofenac, quinidine, rifampicin and ketoconazole).

Considering that the elastic properties of the liver depend on its physiological state, Boulais et al. integrated an alginate-based cryogel with controlled stiffness into a hepatic biochip [159]. They successfully managed to obtain a fine-tuned Young's modulus between that of relatively soft, healthy tissue (~4 kPa) and that of a cirrhotic tissue associated with greater stiffness (~ 15

kPa). The hydrogel made it possible to create a 3D microenvironment which, associated with the perfusable culture system, represents a promising tool for reliable *in vitro* model for drug toxicity and efficacy studies [159].

Hydrogels containing cells can even be shaped to form larger structures. For instance, Massa et al. encapsulated the HepG2/C3a cell line in a gelatine methacryloyl (GelMA) hydrogel and constructed a central vessel using a sacrificial agarose fibre (Fig. 5A) [160]. The central vessel was used as a hollow capillary where endothelial cells were seeded and cultured to form a perfusable monolayer. Through this monolayer, nutrients, oxygen media and drugs could diffuse to reach the 3D organized hepatocytes. This vascularized liver tissue model was subsequently used for continuous perfusing flow and the authors assessed the metabolic activity and viability of the cells after being treated with APAP. They found that incorporating vascular components led to an increase in viability of the hepatocytes compared to those that were directly exposed. This can be explained by the delay in the drugs' diffusion due to their passage through the barrier or their metabolization, which may lower their concentration. Massa et al. thus reproduced *in vivo* vascularization which created a more realistic drug response *in vitro* [160].

3.3.4 3D liver OoC using bioprinting

Recently, 3D bioprinting has been used to manufacture organ-on-chip models. Bioprinting is based on using a bio-ink (composed of cells, matrix, and nutrients) which is precisely deposited on a scaffold layer-by-layer to generate a tissue. Thanks to its ability to print multiple materials and cell types simultaneously, with good spatial resolution, and obtain the desired 3D cellular arrangement, bioprinting can facilitate the creation of a biomimetic environment with the biochip. Thus, the combination of bioprinting and organ-on-chip makes it possible to create complex and biomimetic *in vitro* models for simulation, mechanistic and pharmacological modulation [161].

Organ-on-a-chip models often consist of 3D complex structures composed of microchannels, allowing them to replicate the architecture of native tissue and organs. However, it is hard to control the property and microstructure of soft scaffolds. Bioprinting bypasses this drawback by allowing fine-tuning of the mechanical properties, porosity, micro-structure, and polymerization mechanisms of the hydrogel scaffolds [162].

In the last decade, several 3D-printed liver-on-chip models have been developed. Snyder et al. studied the effectiveness of a radioprotective pro-drug by integrating cell printing into a microfluidic device [163]. The printed biochip was composed of a PDMS substrate and a glass cover. Hepatocytes (HepG2) and epithelial cells (M10) were individually embedded in a Matrigel solution then printed within the PDMS substrate into separate chambers and the whole system was then dynamically perfused with a syringe pump. The authors highlighted that their printed microfluidic device was able to maintain the metabolism activities of both cell types [163].

Recently, another liver-on-a-chip platform has been developed by Bhise et al., with hepatic spheroids (HepG2/C3A cells) fabricated via direct bioprinting in a microfluidic bioreactor device (Fig. 5B) [164]. This model consists of liver tissue printed directly into a microfluidic device which is then assembled around the bioprinted tissue, and serves as a bioreactor to maintain long-term viability (30-day culture period). During the 30 days of culture, the HepG2/C3A spheroids remained functional (albumin, alpha-1 Antitrypsin and transferrin secretions) and exhibited major hepatocyte markers (cytokeratin 18, MRP2 bile canalicular protein and tight junction protein ZO-1). Further, this device bypasses a major drawback of microfluidics by being easily disassembled and reassembled, thus allowing access to the cells over the course of the experiment [164,165].

Fig. 5

3.4 Contribution of OoC technology to the improvement of *in vitro* liver models

The zonation of the hepatocytes in the liver sinusoid is a key feature of the liver characterized by a gradient of activities and functions along the lobule. This gradient remains rarely if ever reproduced in conventional in vitro static cultures [13]. In contrast, microfluidic systems offer the ability to achieve a stable gradient mimicking liver zonation, especially for oxygen which play a key role in metabolic zonation [12]. The dynamic flow allows the delivery of oxygen throughout culture medium perfusion and the diffusion (under laminar flow) creates the oxygen gradient [13]. To improve and accurately control oxygen supply and diffusion in a microfluidic device, two main approaches are used: engineering and chemical approaches [166]. In engineering approach, the oxygen diffusion is controlled by combining oxygen-permeable (PDMS) and -impermeable (e.g., glass, PMMA, PS and PC) materials to build the microfluidic device [166–168]. The chemical approach involves adding oxygen or oxygen scavenging/generating chemicals to the perfused fluid [166,169]. OoC technology allows also the control of chemicals and hormones gradients to generate metabolic zonation [13,170]. Other advantages of the dynamic flow in OoC include the ability to provide controlled shear stress emulating the in vivo mechanical stimulus applied by blood flow on cells and the regulation of drugs/metabolites concentrations, which facilitated drug screening [13].

The liver is composed of several cell types that interact with each other to maintain physiological functions. Therefore, coculture approaches are recommended to build relevant liver models. Unlike conventional culture methods, the advances in microfabrication techniques make the OoC technology suitable for co- or multi-culture of several cell types, while maintaining cell-cell interactions via the fluid perfusion [171]. Among the relevant models, several groups have developed liver OoC devices integrating porous membrane hosting LSECs and mimicking endothelial barrier [172–174]. These devices consist of two compartments separated by the porous membrane. The hepatocytes are generally hosted in the bottom chamber, whereas LSECs are cultivated in the perfused top chamber (upon the membrane) and allow the diffusion of nutrients and chemicals to hepatocytes.

In drug development and chemical risk assessment, the reproduction of ADMET (absorption, distribution, metabolism, excretion and toxicity) process is crucial to validate the safety and/or

efficacy of the target molecule [175]. This process (ADMET) cannot be recreated with the conventional in vitro screening tools such as Petri dish and multi-well plate. Thanks to the fluidic flow, OoC technology allows the recreation of multiorgan interactions. In such multi-OoC platform, the different organs are cultured in separate biochips/compartment and connected together through microfluidic tubing or microchannels [89]. As the centre of chemicals/drug metabolism, the liver is present in the majority of multi-OoC reported in the literature [13,85,89].

4 Liver OoC for toxicity studies

Several research works have been carried out on establishing liver-on-chip models to predict chemical toxicity. The main challenge encountered when developing these models is to recreate the *in vivo* microenvironment of the cells. Knowing that hepatocytes rapidly dedifferentiate when cultured *in vitro*, optimizations have been proposed to maintain their differentiation state and the maintenance of their functions, especially the metabolization of drugs/xenobiotics in an *in vivo*-like situation. Several parameters should be taken in consideration when developing a microfluidic system for hepatocyte culture [176]. The microfluidic system should be adapted for 3D cultures due to the advantages it confers in the promotion of cell-cell and cell-matrix interactions. In addition, the system should be suitable for the co-culture of different cell types, such as fibroblasts and endothelial cells which enhance hepatocyte functions [177]. A non-exhaustive list of measurements has been assessed by Baudy et al., to build a relevant liver *in vitro* model [178]. The aim is to set up fundamental target thresholds to ensure that adequate quantities of metabolites are generated during drug testing. The first stage of the model validation process consists of characterizing performances by measuring albumin, urea and gene expression of the key metabolizing phase I/II enzymes and transporters over 14 days. Once the model passes this step it undergoes the second stage, which consists of assessing the predominant metabolizing enzymes and transporter functions, morphology, cytokine stability and the integrity of hepatobiliary networks. The result of these evaluations then either supports or rejects proceeding to the third stage where

different compounds are tested to evaluate the sensitivity of the model for detecting major mechanistic categories of human hepatotoxicity [178].

4.1 Drug toxicity studies

4.1.1 Drug-induced liver Injury (DILI)

DILI is a common cause of liver injury and accounts for approximately 50% of cases of acute liver failure [113]. It occurs with an incidence ranging from 1 in 10 000 to 1 in 100 000 people, and it is the most common cause for drugs being withdrawn from the market and restricted for use [124]. The severity to DILI depends on the duration of exposure and the histological location of the injury. Depending on these factors, DILI can be considered acute or chronic, and manifests as hepatitis, cholestasis, or a mixed injury. The most important event in hepatitis is necrosis of the hepatocyte.

The first event occurring in DILI consists of inhibition of the mitochondrial respiratory chain. This inhibition causes an accumulation of the reactive oxygen species (ROS) and decreases adenosine triphosphate (ATP). In addition, the damage caused by toxic drugs inhibits the oxidation of fatty acids, which may cause steatosis or steatohepatitis [179]. The association between these 3 events induces intracellular damage and leads to hepatocyte apoptosis. As apoptosis requires ATP, which is depleted because of the mitochondrial dysfunction, hepatocyte death follows a necrotic pathway, leading to hepatic inflammation [180].

The severity of DILI cases depends on the pathologies the liver is predisposed to and its sensitivity to the drugs that are metabolized. For example, hepatitis B, C, and non-alcoholic fatty liver disease (NAFLD) have been associated with increased susceptibility to the inflammatory reactions to the medication [181,182]. In addition, genetic factors predisposing patients to DILI have been identified as affecting polymorphisms on the cytochrome P450 enzymes which slow down either the metabolism of toxic drugs or increase the generation of bioactive metabolites. Every class of medication can cause acute DILI that can be resolved by withdrawing the offending agent [183].

The failure to detect DILI during the drug development process can be attributed to the poor predictability of the screening methods (*in vitro*, *in vivo*, *ex vivo* and *in silico*) used in the preclinical phase [113]. Current models are unreliable for detecting DILI due to the complex interactions implied in the genesis of DILI itself. In addition, these interactions imply genetic, non-genetic, and environmental factors that most of these models fail to recreate. The liver organ-on-chip models are emerging as an alternative solution for predicting hepatotoxicity thanks to the flexibility they confer (possibility of recreating a controlled cellular micro environment) and the possibility of studying acute and chronic exposure to toxicants while maintaining cellular functionalities [124].

4.1.2 Liver organ-on-chip model for drug toxicity

The pharmaceutical development of drugs is considered very costly ($2.6 billion per marketed drug) and inefficient (94% of drugs fail clinical trials) [165]. The most common cause of drug withdrawal during the clinical phase is drug-induced toxicity, caused by the low predictability of human liver toxicity. The battery of tests used for the marketing of potentially bioactive molecules requires the use of animal models for drug toxicity assays. As an alternative, researchers are starting to promote the potential of organ-on-chip-based platforms, essentially liver-on-chip due to the correlation between drug toxicity and hepatotoxicity, as an *in vitro* model for drug toxicity studies [165]. In past decades, a variety of liver OoCs have emerged for different applications, including toxicity studies, studying metabolism, and disease modelling. Below, we review the applications of liver OoC in drug toxicity studies. We have also summarized in Table 1 the main liver OoC models reported for drug toxicity studies.

Snouber et al. investigated the toxicity of flutamide, an anticancer prodrug, and its toxic metabolite hydroxyflutamide on the HepG2/C3a cell line cultured in a PDMS biochip coated with fibronectin [184]. The metabolic activity of HepG2/C3a has been analysed by full metabolomic profiling. They observed a hepatotoxic reaction for the exposed group, illustrated by disrupted glucose homeostasis and mitochondrial dysfunctions compared to the non-

exposed control group. In addition, the production of the toxic metabolite (hydroxyflutamide) led to specific mechanistic toxic signatures correlated with hepatotoxicity. Using the model designed, Snouber et al., proposed a list of biomarkers describing glutathione depletion, caused by both molecules' hepatotoxicity, which is followed by the death of the HepG2/C3a cells. Using the same liver biochip, Prot et al. investigated acetaminophen (APAP) toxicity on HepG2/C3a cells using a proteomic and transcriptomic approach [185]. They observed an induced NRF2 pathway and enhanced drug-related metabolism pathways. In addition, exposure to APAP provoked inhibited cell growth and a metabolic signature of APAP toxicity correlated with *in vivo* situations, such as modulated calcium homeostasis, lipid metabolism, and reorganization of the cytoskeleton. On the other hand, omics profiling revealed disturbances in DNA replication and the cell cycle in both the biochip and Petri dishes when exposed to APAP. Their research demonstrated the potential of microfluidic biochips as a tool for investigating drug toxicity studies.

To improve prediction of human hepatotoxicity, it is important to take into consideration *in vivo*-like hepatocyte organization and cell-matrix interactions. As described in Section 3.3, different approaches have been used to promote the 3D organization of the cells inside microfluidic systems. Zuchowska et al. investigated the effect of 5-fluorouracil (5-FU, an anticancer drug) on HepG2 spheroids formed in a microfluidic system integrating U-shaped designs (Fig. 6A) [186]. The intention to work with spheroids comes from their similarity to an early, vascular stage of tumours, which makes them an appropriate model for evaluating the cytotoxic properties of compounds. To obtain the HepG2 spheroid, the cells were seeded in a PDMS-based biochip composed of concave chambers and channels and, depending on the number of cells seeded, different spheroid diameters were obtained. They then correlated between the cross-sectional spheroid areas, which indicated the death or proliferation rate of the cells, and the cytotoxic effect of 5-FU. They observed a decrease in the cross-sectional area when the cells were treated with different concentrations of 5-FU. In addition, by evaluating the effect of the drug for 10 days, starting on the 8th day of exposure, the HepG2 spheroids acquired drug resistance for 5-fluorouracil. This phenomenon can only be noticed in the microfluidic systems,

demonstrating the potential of the model designed by Zuchowska et al. for predicting drug resistance. Another application of the HepG2 spheroid-on-chip model for drug toxicity is the work by Knowlton et al.,[165] and Bhise et al.,[164] who developed a liver tissue model using a bioprinting approach for hepatic spheroids encapsulated in a hydrogel scaffold. The HepG2/C3a spheroids were assembled using a microwell technique then suspended in a gelatine methacryloyl (GelMA) hydrogel scaffold. Then, using a bioprinter, the spheroids were directly injected into the microfluidic device, forming liver tissue. By exposing these spheroids to an acute, toxic dose of APAP, they observed a significant decrease in both metabolic activity and cell density. The results obtained from this acute toxic exposure were correlated with similar animal and *in vitro* exposure models, confirming the potential for applying the model developed in drug toxicity analyses.

Hepatocyte cell lines have limited metabolic activity, which is a crucial feature when developing hepatic models for drug toxicity assessment. To overcome this limitation, Yu et al. used rat hepatocyte spheroids to evaluate the chronic drug response to diclofenac and acetaminophen in a liver-on-chip bioreactor (Fig. 6B) [187]. The pre-formed hepatocyte spheroids were introduced into the biochip and compared with a collagen sandwich culture as the standard. By measuring the metabolism of phenacetin, bupropion, and midazolam, and the production of their metabolites: acetaminophen, OH-bupropion and OH-midazolam respectively, they observed enhanced hepatic functions that were correlated with the activity of CYP1A2, CYP2B1/2 and CYP3A2. In addition, the model was used to test the acute and chronic toxicity of diclofenac and APAP, and was found to be more sensitive in testing the chronic drug response. The toxic effect was only observed after 14 days of exposure and viability was significantly reduced compared to the collagen sandwich control.

One of the main challenges when developing a biomimetic liver model is ensuring its accuracy in predicting the toxicity of candidate drugs. Using rodent and non-rodent toxicity models may produce discordant results or fail to predict toxicity in humans. In the same context, Jang et al. designed a liver-chip containing species-specific rat, dog, and human primary hepatocytes co-cultured with liver sinusoidal endothelial cells, with and without Kupffer and hepatic stellate

cells [188]. The biochip was composed of 2 channels separated by a porous membrane. The upper channel hosted rat, dog, and human hepatocytes within an ECM-coated sandwich, and the lower channel contained species-specific liver endothelial cells, with or without Kupffer cells and/or stellate cells. By testing the toxicity of bosentan, a drug known to provoke DILI in humans but not in rats or dogs, they observed a hepatotoxic effect in the human liver-chip corresponding to the toxic plasmatic concentration which correlated the liver-chip response with the clinical response. In addition, the toxic concentration affected albumin secretion in humans and dogs, but not rats, which correlated with *in vivo* findings. Using the multispecies liver-chip detected the hepatotoxicity of bosentan more accurately than conventional sandwich monoculture plates. In addition to bosentan, after integrating species-specific nonparenchymal cells (NPC), hepatic stellate and Kupffer cells into the vascular channel, they tested the hepatotoxic effect of acetaminophen. They observed depletion of glutathione (GSH) and adenosine 5'-triphosphate (ATP) preceded by a decline in hepatocyte morphology and function. These results were confirmed by the decrease in albumin synthesis and the increase in oxidative stress-related markers.

Massa et al. successfully incorporated an engineered endothelial cell layer using human umbilical vein endothelial cells (HUVEC) in a 3D liver construct created with HepG2/C3a cells encapsulated in gelatine methacryloyl (GelMA) hydrogel (Fig. 4C) [160]. By continuously perfusing the vessel construct with APAP mixed with HUVEC culture media, they observed a decrease in HUVEC metabolic activity, viability, and damage disturbing confluency and the endothelial monolayer. In addition, when integrating the HepG2/C3a liver tissue, the APAP treatment resulted in cell death near the channel and higher viability in the vicinity of the channel. These results were correlated with those obtained when working with *ex vivo* models. The integration of the HUVEC layer makes the model suitable for drug testing and promote the role of integrating vascularisation for their role in delaying the diffusion of drugs. Indeed, the HUVEC layer formed a barrier mimicking the in vivo drug administration process. in addition to their potential metabolic role for some drugs.

Fig. 6

4.2 Liver OoC for environmental and other toxicant studies

An environmental toxicant is any molecule produced by humans or introduced into the environment by human action. Toxicants represent a threat to human health, especially after long-term exposure [189]. They can attain the human body through the skin, inhalation or ingestion, and be translocated to other organs by diffusion or transportation via the blood and lymph. Environmental toxicants can be classified into four major groups: natural toxins, heavy metals, endocrine-disrupting chemicals (EDCs), and nanomaterials [86,190]. Human exposure to environmental toxicants is mainly chronic through daily exposure to low doses (residues) of complex cocktails of toxicants present in the food supply, soil, water, atmosphere and agricultural products [191]. In risk assessment, most commonly, animal models or *in vitro* 2D cell cultures in Petri dishes are used. However, animal models lose their relevance when extrapolating the results to humans, and static cultures using conventional Petri dishes are poorly predictive and not suitable for long-term cultures (chronic studies). Due to their inherent advantages, such as a relevant physiological microenvironment and maintenance of long-term functionality, liver OoC systems offer a powerful approach for risk assessment of environmental toxicants. However, although liver OoC technology has been widely used for drug toxicity screening, only a few works have reported their use in environmental toxicology assays [86] (summarized in Table 1).

Endocrine-disrupting chemicals (EDCs) are exogenous chemicals, such as pesticides and herbicides, that mimic, block, or interfere with endogenous hormones and other signalling chemicals in the endocrine system [192]. The widespread application of pesticides in the farming sector has contributed to the pollution of drinking water sources, vegetables, cattle food, milk, and fish. Dichlorodiphenyl- trichloroethane (DDT) and permethrin (PMT) are among the most prevalent pesticides in the environment and have been implicated in the development of different chronic diseases. DDT and PMT have been associated with dysregulation of liver lipids and glucose metabolism, and non-alcoholic fatty liver disease (NAFLD) [193,194]. Jellali et

*a*l. used a rat liver organ-on-chip model coupled to multi-omics to investigate the liver damage induced by DDT, PMT and their combination (Fig. 7A). The transcriptome and metabolome analysis highlighted a dose-dependent effect for all conditions, with a profile close to the control condition for low doses of pesticides. Furthermore, transcriptome modulation reflected liver inflammation, steatosis, necrosis, *PPAR* signalling and fatty acid metabolism [191,195,196]. Rotenone is a widely used organic pesticide known to induce oxidative stress and the mitochondrial dysfunction involved in the pathogenesis of Parkinson's disease [197,198]. Bavli et al. developed a liver-on-chip model capable of maintaining 3D aggregates of HepG2/C3A cells for 28 days while monitoring oxygen uptake, glucose uptake, and lactate production rates over the same period. They noticed damage to respiratory cells directly after exposure to rotenone, in addition to an increase in cellular death and a drop in glucose uptake after 6h. Thus, their platform was able to monitor metabolic changes indicating mitochondrial and metabolic dysfunction after exposure to pesticides [199].

Nanomaterials are very small materials that are 10000 times smaller than the thickness of a human hair. This small size gives them physical and chemical properties different from those of "traditional" materials. Despite the widespread use of these nanomaterials in cell/tissue engineering and pharmacological/medical device development, knowledge of the toxicity and potential health risks associated with using nanomaterials remains extremely limited. Superparamagnetic iron oxide nanoparticles (SPION) are currently the only clinically approved metal oxide nanoparticles and the most used superparamagnetic nanoparticles [200,201]. A microfluidic 3D liver-on-chip with three material layers, which contains primary rat hepatocytes, has been fabricated and tested using different concentrations (50, 100 and 200 µg/ml) of SPION for 3-day (short-term) and 1-week (long-term) cultures. Compared to static culture, the liver-on-chip with flow provided comparable viability and significantly higher liver-specific functions, up to 1-week. Moreover, the dynamic culture made it possible to mimic real cumulative exposure to SPION by minimizing possible agglomeration of the molecule, which caused more harmful effects in liver-specific functions (albumin and urea secretion) and viability, in a dose- and time-dependent manner (Fig. 7B) [202]. Recently, another study explored

the hepatotoxicity of copper sulphide nanoparticles (CuSNPs) using hepatocyte spheroids in a multi-concave agarose chip. Exposure to CuSNPs caused a decrease in spheroid viability and hepatocyte-specific functions, such as albumin/urea production, glycogen deposits, and hepatobiliary transport. Moreover, alteration to mitochondrial membrane potential and increased production of reactive oxygen species demonstrated hepatocyte damage [203].

Some molecules, although not toxic to humans in moderate quantities, can become so when overexposed. For instance, ethanol, which is the main component of alcoholic beverages and also present in many pharmaceuticals and cosmetic products, has become a target for toxicologists. Alcohol is the main cause of liver diseases as it is metabolized in the liver. Thus, developing *in vitro* models mimicking *in vivo* liver physiology is essential for understanding the mechanisms of alcoholic liver disease (ALD) and implementing treatment method. For this purpose, spheroids composed of rat primary hepatocytes and hepatic stellate cells (HSCs) were cultured in a fluidic chip to investigate the role of HSCs in livers with ALD, and an interstitial level of flow was applied to the chip to provide *in vivo* mimicking fluid activity [204]. Hepatic function assessment showed lower albumin secretion and enzyme activity in the ethanol-treated group than in the control. Outcomes also demonstrated that HSCs were activated and contributed to the ALD process.

Fig. 7

Table 1

5 Multi-organ-on-chip model integrating liver for chemical-induced toxicity

The liver is interconnected to other organs or tissues by means of complex biological mechanisms that cause a complex global response upon exposure to xenobiotics. Traditional cell culture models mainly target a single organ or tissue and do not reproduce this level of complexity. Microphysiological system technology, which relies heavily on microfabrication and microfluidics, is ideal for mimicking such interactions in a reductionist way, by connecting and integrating multiple organs in a unique system. These multi-organ systems, termed as multi-organ-on-chip (multi-OoC), have emerged as potential tools for studying the toxicity of

both drugs and environmental pollutants [83]. Table 2 summarizes various MOS systems integrating the liver and used for toxicity studies.

Drug-induced hepatotoxicity and nephrotoxicity are two major risks for human health. Theobald et al. designed a microsystem device composed of two interconnected chambers, for hepatic (HepG2) and kidney (Hek293) cells, making it possible to study both organs after exposure to toxins and drug (aflatoxin B1 (AFB1), benzo-alpha-pyrene (BαP) and rifampicin). AFB1 and BαP are known to induce primary toxicity in the liver leading to the production of epoxide, which is responsible for toxicity in other tissues and organs. The authors highlighted that xenobiotic metabolism-associated biomarkers of hepatic cells including albumin, urea, and CYPs were more stably and highly expressed under fluidic conditions. They also demonstrated the ability of this liver-kidney-on-chip device to support liver-kidney communication and reproduce the bioactivation, metabolism and clearance of both toxins and drugs [210].

The first pass metabolism illustrating the passage of chemicals/drugs through the intestines to the liver is important in determining the effects of xenobiotics and understanding their mechanism of action [13]. Marin et al. developed a two-organ-chip platform to culture the intestines and liver for studying the absorption and metabolism of APAP [211]. The intestinal barrier was produced by Caco-2 and HT-29 cells on a culture insert and the liver spheroids were produced with HepaRG and HHSTeC cells using the hanging drop technique and cultivated in the hepatic compartment. To mimic APAP absorption through the intestinal barrier, Marin et al. used two concentrations of APAP corresponding to oral and intravenous administration in the apical side and measured its passage through the barrier. *In vivo*, APAP is largely absorbed through the intestines but its toxic metabolites are only generated in the liver. The same phenomenon was observed with the model by Marin et al. when measuring the production of N-acetyl-p-benzo-quinone, a hepatotoxic metabolite of APAP. In addition, they obtained a similar absorption curve and metabolism phases to the classic bioavailability curve obtained *in vivo* for most drugs. Intestine-liver microsystems can also be used for environmental toxicity assessment. Esch et al. simulated the oral uptake of a 50 nm

carboxylated polystyrene nanoparticle with a gastrointestinal tract-liver-other tissue microsystem [212]. They determined that ingestion of carboxylated polystyrene nanoparticles, even in low concentrations, cross the GI tract epithelium and affect liver tissue. They noticed an increase in aspartate aminotransferase (AST) levels in the culture medium despite the absence of a significant decrease in cell viability, suggesting transient and sublethal cell injury. MOC may also improve the toxicological assessment of aerosols that have been implicated in the development of chronic obstructive pulmonary disease, asthma, or lung cancer. For this reason, Bovard et al. designed an acute and chronic toxicity study on a lung/liver biochip. The microsystem was composed of an air-liquid interface (ALI), where normal human bronchial epithelial (NHBE) cells were cultured, and a liver compartment with HepaRG™ spheroids. The capacity of liver cells to metabolize and regulate toxicity was assessed using AFB1. Outcomes showed that after 48 hours of exposure, AFB1 toxicity on NHBE ALI tissues decreased in co-culture conditions, proving that the HepaRG™-mediated detoxification protected/decreased from AFB1-mediated cytotoxicity [213]. In this same approach, Schimek et al. designed a HUMIMIC Chip3plus which included a large medium reservoir, an air-permeable membrane above the lung culture compartment to ensure optimal air circulation, and a liver compartment composed of HepaRG and primary human hepatic stellate cell (HHSteCs) spheroids (Fig.8A) [214]. Thanks to the AFB1 treatment, they demonstrated crosstalk in the lung-liver coculture. After 24h of exposure, they observed a slight decrease in cell functionality and viability in the co-culture system in comparison to monoculture bronchial MucilAir. These results suggest a protective role for the liver spheroids which decreased AFB1 toxicity by metabolizing it. Moreover, a decrease in albumin production was observed, indicating hepatocyte alteration. This study thus reproduces and corroborates the findings reported by Bovard et al. [213]. Naphthalene, a pesticide used as an insecticide and repellent, has also been studied. Viravaidya et al. described the application of a two-cell system, four-chamber µCCA (Cell Culture Analogue) device composed of lung, liver, fat and other tissue for an *in vitro* ADMET study of naphthalene [215]. The study highlighted that naphthalene is metabolized by the liver into reactive metabolites which then circulate to the lung, causing glutathione depletion leading

to oxidative stress and lung cell death [215,216].These studies illustrate the potential of organ-on-chip models for pesticide toxicological studies and provide new tools for chemical risk assessment. Therefore, the lung/liver-on-a-chip platform presented here offers new opportunities for studying the toxicity of inhaled aerosols, such as toxins or pesticides, and/or new drug candidates targeting the lungs.

Although drug toxicity mainly causes acute liver failure, it can also induce alterations in the brain as secondary effects. Studies have been conducted to determine drug-metabolized response in the brain. Materne et al. developed an MOC capable of maintaining in culture 3D spheroids of neurospheres derived from undifferentiated NT2 cells and liver cells (HepaRG and primary human hepatic stellate cells) [217]. They observed that exposure to the neurotoxic 2,5-hexanedione induced higher apoptosis rates within neurospheres and liver tissues in monoculture, when compared with the neurosphere-liver co-culture. Therefore, these outcomes suggest that single-tissue organ-on-chips are less predictive and accurate than multi-organ-on-chips. The liver-brain chip may also be useful for assessing the metabolism of drug candidates for certain neuropathologies. Li et al. designed a multi-interface liver-brain chip composed of three microchannels separated by a porous membrane and collagen to assess hepatic metabolism-dependent cytotoxicity of anti-brain-tumour drugs [218]. HepG2 and U87 cells were cultured in separate channels to mimic the liver and glioblastoma, while brain microvascular endothelial cells (BMECS) and cerebral astrocytes were co-cultured on collagen to mimic the blood-brain-barrier (BBB). They evaluated the physiological process of three common anti-tumour drugs: paclitaxel (PTX), capecitabine (CAP) and temozolomide (TMZ). Their results highlighted that the liver compartment enhanced the cytotoxicity of CAP on U87 cells but had no significant effect on TMZ. On the other hand, the BBB decreased the cytotoxicity of PTX, while no significant effects were observed on TMZ and CAP. These results demonstrated the importance of liver metabolism and the blood–brain barrier for evaluating anti-brain-tumour drugs and the potential of liver-brain-chips for evaluating anti-brain-tumour drugs in a more accurate manner [218].

One of the most important targets of the toxic metabolites produced by the liver is the heart. To understand the dynamic interactions between these two organs, liver-heart models have been developed to predict off-target cardiac toxicity on liver metabolism. Soltantabar et al. 2021 developed a heart-liver-chip using HepG2 cells and H9c2 rat cardiomyocytes to test the toxicity effect of doxorubicin (Fig. 8B) [219]. The cardiotoxic effect of doxorubicin is due to its primary metabolite, doxorubicinol. The PDMS biochip was composed of 2 culture chambers interconnected by fluidic channels. After drug treatment, they observed the appearance of the cardiotoxic metabolite, doxorubicinol, and its toxic effect was confirmed by quantifying the viability of the cardiac cells within the model. They observed a significant difference in the apoptotic cells in the device compared to static culture. The model by Soltantabar et al. promotes the potential of multi-organ-on-chip models for evaluating the toxicity of both the parent drug and its metabolites and the effect on both organs [219].

Fig. 8

Table 2

6 Conclusion and future challenges

Over the past few decades, liver OoC technology has undergone significant progress and has now become a promising *in vitro* test system for different applications, especially in drug toxicity screening and environmental risk assessment. The significant advancements in tissue engineering, biomaterials, design and microfabrication, stem cell technologies and knowledge of the liver microenvironment make it possible to build liver OoC with highly complex and specific cellular architectures. Thanks to the use of bioprinting, organoid technology and hydrogels/hydroscaffolds, it is possible to construct vasculature and 3D architecture, as well as to model mechanical properties, cell-cell and cell-ECM interactions. The evolution in perfusion systems makes possible precise control of media flow reproducing flow, mechanical stimuli and dilutions of metabolites and paracrine signals similar to those in physiological situations. Currently, liver OoC benefits from the iPSC technology that provides a readily-available human cell source and makes it possible to develop multicellular liver OoC

(hepatocytes + NPCs) using cells from the same donor (same genetic background). Such developments, coupled with easy imaging and the possibility of incorporating biosensors and connecting OoC to analytical tools, make liver OoC technology a powerful tool for both replacing the traditional “black box” of animal-based and conventional 2D *in vitro*-based paradigms, and promoting the implementation of the '3Rs' (replacement, reduction, and refinement of animal models).

Although it is recognized today that the liver OoC models will replace many animal experiments, many obstacles still need to be addressed in the future. PDMS is the most widely used material for constructing liver OoC. PDMS absorbs hydrophobic molecules and is not suitable for tests using drugs/chemicals. With the progress made in microfabrication and 3D printing, a variety of devices with new materials have been proposed [91,97,222]. However, detailed comparisons of these devices with PDMS-based biochips, including biological performances/functions, long-term cultures, interactions with cells and molecules, and utility as pharmacokinetic models are needed to validate their use in toxicology studies and drug screening.

Cell sourcing is one of the keys to the development of relevant liver OoC models. Primary human cells have limited availability and display inter-donor variability, whereas lines, used for their reproducibility, fail to replicate tissue-specific functions in vivo-like metabolic activity [82]. Human iPSC-derived hepatocytes provide great cell sources for liver OoC. Nevertheless, the protocols for hiPSC differentiation lead to immature and heterogeneous hepatocytes. Furthermore, only very few protocols are available for iPSC differentiation into NPCs, which are essential for construction of relevant multicellular liver OoC. The protocols for iPSC differentiation into hepatocytes and NPCs need to be further explored to obtain highly mature hepatic cells. The choice of appropriate culture medium is also crucial factor in liver OoC development, especially for coculture of different types of liver cell and multi-OoC integrating liver OoC with other organs. Currently, there is no universal medium for culture of multiple cells or organs. Most commonly, mixtures of culture media or common media (such as MEM, DMEM and William’s medium) supplemented with components specific for each cell types are

used [88,89]. However, these strategies can lead to strong medium interactions and lower concentrations of individual components, and are not suitable for a variety of cells, especially primary cells and iPSCs that are sensitive to the culture environment [223]. Overall, it is clear that complex development including biological optimizations, engineering efforts and advanced characterizations are necessary to identify common culture medium for a large variety of cells.

The other major challenges for OoC technology are standardization and compatibility with standard laboratory equipment [224]. To address these issues, several initiatives and consortia involving the OoC community, pharmaceutical companies, academic researchers, and standards development organisations (SDOs) have emerged in recent years. These actions have been reinforced by recognition of the potential for OoC technology and increasing financial support from the European Union (EU), the United States, and the Japanese government for project related to OoC [84,225].

Acknowledgements

The authors thank the ANR (Agence National de la Recherche, MIMLIVEROnChip ANR-19-CE19-0020-01 project) and the French Ministry of Higher Education and Research for their financial support through the PhD grants of Taha Messelmani and Lisa Morisseau.

Conflicts of interest

There are no conflicts of interest to declare.

References

1 A. Kalra, E. Yetiskul, C. J. Wehrle and F. Tuma, *StatPearls*.

2 X. Gu and J. E. Manautou, *Expert Rev Mol Med*, 2012, **14**, e4.

3 O. B. Usta, W. J. McCarty, S. Bale, M. Hegde, R. Jindal, A. Bhushan, I. Golberg and M. L. Yarmush, *https://doi.org/10.1142/S2339547815300012*, 2015, **03**, 1–26.

4 D. E. Malarkey, K. Johnson, L. Ryan, G. Boorman and R. R. Maronpot, *Toxicologic Pathology*, 2005, **33**, 27–34.

5 J. Deng, W. Wei, Z. Chen, B. Lin, W. Zhao, Y. Luo and X. Zhang, *Micromachines 2019, Vol. 10, Page 676*, 2019, **10**, 676.

6 J. Poisson, S. Lemoinne, C. Boulanger, F. Durand, R. Moreau, D. Valla and P. E. Rautou, *J Hepatol*, 2017, **66**, 212–227.

7 S. Shetty, P. F. Lalor and D. H. Adams, *Nature Reviews Gastroenterology & Hepatology 2018 15:9*, 2018, **15**, 555–567.

8 J. H. Lefkowitch, *Scheuer's Liver Biopsy Interpretation*, 2016, 383–403.

9 I. Bykov, P. Ylipaasto, L. Eerola and K. O. Lindros, *Comparative Hepatology 2004 3:1*, 2004, **3**, 1–3.

10 C. H. Beckwitt, A. M. Clark, S. Wheeler, D. L. Taylor, D. B. Stolz, L. Griffith and A. Wells, *Experimental Cell Research*, 2018, **363**, 15–25.

11 S. S. Bale and J. T. Borenstein, *Drug Metabolism and Disposition*, 2018, **46**, 1638–1646.

12 T. Kietzmann, *Redox Biology*, 2017, **11**, 622–630.

13 S. Y. Lee, D. Kim, S. H. Lee and J. H. Sung, *APL Bioengineering*, 2021, **5**, 041505.

14 R. Gebhardt, *Pharmacology & Therapeutics*, 1992, **53**, 275–354.

15 M. Hundt, H. Basit and S. John, *StatPearls*.

16 R. N. Moman, N. Gupta and M. Varacallo, *StatPearls*.

17 *LiverTox: Clinical and Research Information on Drug-Induced Liver Injury*.

18 A. Kalra, E. Yetiskul, C. J. Wehrle and F. Tuma, *StatPearls*.

19 C. J. Omiecinski, J. P. vanden Heuvel, G. H. Perdew and J. M. Peters, *Toxicological Sciences*, 2011, **120**, S49–S75.

20 O. A. Almazroo, M. K. Miah and R. Venkataramanan, *Clin Liver Dis*, 2017, **21**, 1–20.

21 N. B. Sandson, *A Case Approach to Perioperative Drug-Drug Interactions*, 2015, 57–60.

22 J. H. Lewis and D. E. Kleiner, *MacSween's Pathology of the Liver*, 2012, 645–760.

23 V. Y. Soldatow, E. L. Lecluyse, L. G. Griffith and I. Rusyn, *Toxicol Res (Camb)*, 2013, **2**, 23.

24 M. R. McGill and H. Jaeschke, *Biochim Biophys Acta Mol Basis Dis*, 2019, **1865**, 1031.

25 T. J. Bateman, V. G. B. Reddy, M. Kakuni, Y. Morikawa and S. Kumar, *Drug Metabolism and Disposition*, 2014, **42**, 1055–1065.

26 J. R. Foster, G. Lund, S. Sapelnikova, D. L. Tyrrell and N. M. Kneteman, *Xenobiotica*, 2014, **44**, 109–122.

27 Y. W. Son, H. N. Choi, J. H. Che, B. C. Kang and J. W. Yun, *Regulatory Toxicology and Pharmacology*, 2020, **116**, 104757.

28 H. Prior, P. Baldrick, L. de Haan, N. Downes, K. Jones, E. Mortimer-Cassen and I. Kimber, *International Journal of Toxicology*, 2018, **37**, 121.

29 Smith David and Trennery Paul, *Non-Rodent Selection in Pharmaceutical Toxicology*, 2002.

30 P. Barrow, *Reproductive Toxicology*, 2016, **64**, 57–63.

31 G. Schmitt, P. Barrow and M. Stephan-Gueldner, *The Nonhuman Primate in Nonclinical Drug Development and Safety Assessment*, 2015, 337–355.

32 M. Martignoni, G. M. M. Groothuis and R. de Kanter, *Expert Opin Drug Metab Toxicol*, 2006, **2**, 875–894.

33 T. Nakamura, K. Fujiwara, M. Saitou and T. Tsukiyama, *Stem Cell Reports*, 2021, **16**, 1093–1103.

34 A. E. M. Vickers and R. L. Fisher, *Applied In Vitro Toxicology*, 2018, **4**, 280–287.

35 J. van Delft, K. Mathijs, J. Polman, M. Coonen, E. Szalowska, G. R. Verheyen, F. van Goethem, M. Driessen, L. van de Ven, S. Ramaiahgari and L. S. Price, *Toxicogenomics-Based Cellular Models*, 2014, 193–212.

36 D. Kartasheva-Ebertz, J. Gaston, L. Lair-Mehiri, P. P. Massault, O. Scatton, J. C. Vaillant, V. A. Morozov, S. Pol and S. Lagaye, *World Journal of Hepatology*, 2021, **13**, 187.

37 A. Guillouzo, *Environmental Health Perspectives*, 1998, **106**, 511–532.

38 Z. Li, *Comprehensive Biotechnology, Second Edition*, 2011, **5**, 551–563.

39 L. Díaz, E. Zambrano, M. E. Flores, M. Contreras, J. C. Crispín, G. Alemán, C. Bravo, A. Armenta, V. J. Valdés, A. Tovar, G. Gamba, J. Barrios-Payán and N. A. Bobadilla, *Revista de investigacion clinica; organo del Hospital de Enfermedades de la Nutricion*, 2020, **73**, 199–209.

40 K. Jaroch, A. Jaroch and B. Bojko, *Journal of Pharmaceutical and Biomedical Analysis*, 2018, **147**, 297–312.

41 I. de Angelis, L. Ricceri and A. Vitale, *Annali dell'Istituto superiore di sanita*, 2019, **55**, 398–399.

42 P. Godoy, N. J. Hewitt, U. Albrecht, M. E. Andersen, N. Ansari, S. Bhattacharya, J. G. Bode, J. Bolleyn, C. Borner, J. Böttger, A. Braeuning, R. A. Budinsky, B. Burkhardt, N. R. Cameron, G. Camussi, C. S. Cho, Y. J. Choi, J. Craig Rowlands, U. Dahmen, G. Damm, O. Dirsch, M. T. Donato, J. Dong, S. Dooley, D. Drasdo, R. Eakins, K. S. Ferreira, V. Fonsato, J. Fraczek, R. Gebhardt, A. Gibson, M. Glanemann, C. E. P. Goldring, M. J. Gómez-Lechón, G. M. M. Groothuis, L. Gustavsson, C. Guyot, D. Hallifax, S. Hammad, A. Hayward, D. Häussinger, C. Hellerbrand, P. Hewitt, S. Hoehme, H. G. Holzhütter, J. B. Houston, J. Hrach, K. Ito, H. Jaeschke, V. Keitel, J. M. Kelm, B. Kevin Park, C. Kordes, G. A. Kullak-Ublick, E. L. Lecluyse, P. Lu, J. Luebke-Wheeler, A. Lutz, D. J. Maltman, M. Matz-Soja, P. McMullen, I. Merfort, S. Messner, C. Meyer, J. Mwinyi, D. J. Naisbitt, A. K. Nussler, P. Olinga, F. Pampaloni, J. Pi, L. Pluta, S. A. Przyborski, A. Ramachandran, V. Rogiers, C. Rowe, C. Schelcher, K. Schmich, M. Schwarz, B. Singh, E. H. K. Stelzer, B. Stieger, R. Stöber, Y. Sugiyama, C. Tetta, W. E. Thasler, T. Vanhaecke, M. Vinken, T. S. Weiss, A. Widera, C. G. Woods, J. J. Xu, K. M. Yarborough and J. G. Hengstler, *Archives of Toxicology*, 2013, **87**, 1315.

43 G. Elaut, P. Papeleu, M. Vinken, T. Henkens, S. Snykers, T. Vanhaecke and V. Rogiers, *Methods Mol Biol*, 2006, **320**, 255–263.

44 A. J. Shaw, A. Gescher and J. Mráz, *Toxicol Appl Pharmacol*, 1988, **95**, 162–170.

45 D. Jouin, N. Blanchard, E. Alexandre, F. Delobel, P. David-Pierson, T. Lavé, D. Jaeck, L. Richert and P. Coassolo, *European journal of pharmaceutics and biopharmaceutics : official journal of Arbeitsgemeinschaft fur Pharmazeutische Verfahrenstechnik e.V*, 2006, **63**, 347–355.

46 M. J. Griffin and H. S. Sul, *IUBMB Life*, 2004, **56**, 595–600.

47 B. Andria, A. Bracco, G. Cirino and R. A. F. M. Chamuleau, *Cell Medicine*, 2010, **1**, 55.

48 E. Milner, M. Ainsworth, M. McDonough, B. Stevens, J. Buehrer, R. Delzell, C. Wilson and J. Barnhill, *Medicine in Drug Discovery*, 2020, **8**, 100060.

49 K. Duval, H. Grover, L. H. Han, Y. Mou, A. F. Pegoraro, J. Fredberg and Z. Chen, *Physiology*, 2017, **32**, 266.

50 J. A. Kyffin, P. Sharma, J. Leedale, H. E. Colley, C. Murdoch, P. Mistry and S. D. Webb, *Toxicology in Vitro*, 2018, **48**, 262–275.

51 J. Keemink, M. Oorts and P. Annaert, *Methods in Molecular Biology*, 2015, **1250**, 175–188.

52 X. Liu, J. P. Chism, E. L. LeCluyse, K. R. Brouwer and K. L. R. Brouwer, *Drug Metabolism and Disposition*.

53 R. T. Mingoia, D. L. Nabb, C. H. Yang and X. Han, *Toxicol In Vitro*, 2007, **21**, 165–173.

54 J. C. Y. Dunn, M. L. Yarmush, H. G. Koebe and R. G. Tompkins, *FASEB J*, 1989, **3**, 174–177.

55 M. Norikazu, F. Yukina, I. Haruo and T. Ikumi, *Drug Metabolism and Disposition*, 2018, **46**, 680–691.

56 E. Kimoto, J. Chupka, Y. Xiao, Y. A. Bi and D. B. Duignan, *Drug Metab Dispos*, 2011, **39**, 47–53.

57 T. de Bruyn, S. Chatterjee, S. Fattah, J. Keemink, J. Nicolaï, P. Augustijns and P. Annaert, *Expert Opin Drug Metab Toxicol*, 2013, **9**, 589–616.

58 S. Chatterjee, L. Richert, P. Augustijns and P. Annaert, *Toxicol Appl Pharmacol*, 2014, **274**, 124–136.

59 K. Mathijs, A. S. Kienhuis, K. J. J. Brauers, D. G. J. Jennen, A. Lahoz, J. C. S. Kleinjans and J. H. M. van Delft, *Drug Metab Dispos*, 2009, **37**, 1305–1311.

60 O. Schaefer, S. Ohtsuki, H. Kawakami, T. Inoue, S. Liehner, A. Saito, A. Sakamoto, N. Ishiguro, T. Matsumaru, T. Terasaki and T. Ebner, *Drug Metab Dispos*, 2012, **40**, 93–103.

61 F. Pampaloni, E. Stelzer and A. Masotti, *Recent Patents on Biotechnology*, 2009, **3**, 103–117.

62 V. Hosseini, N. F. Maroufi, S. Saghati, N. Asadi, M. Darabi, S. N. S. Ahmad, H. Hosseinkhani and R. Rahbarghazi, *Journal of Translational Medicine 2019 17:1*, 2019, **17**, 1–24.

63 F. Pampaloni, E. G. Reynaud and E. H. K. Stelzer, *Nature Reviews Molecular Cell Biology 2007 8:10*, 2007, **8**, 839–845.

64 J. P. Chen, S. C. Yu, B. R. S. Hsu, S. H. Fu and H. S. Liu, *Biotechnology Progress*, 2003, **19**, 522–527.

65 H. K. Makadia and S. J. Siegel, *Polymers (Basel)*, 2011, **3**, 1377.

66 W. Han, Q. Wu, X. Zhang and Z. Duan, *Journal of Applied Toxicology*, 2019, **39**, 146–162.

67 A. Skardal, L. Smith, S. Bharadwaj, A. Atala, S. Soker and Y. Zhang, *Biomaterials*, 2012, **33**, 4565–4575.

68 S. Kazemnejad, *Avicenna Journal of Medical Biotechnology*, 2009, **1**, 135.

69 C. C. Bell, D. F. G. Hendriks, S. M. L. Moro, E. Ellis, J. Walsh, A. Renblom, L. Fredriksson Puigvert, A. C. A. Dankers, F. Jacobs, J. Snoeys, R. L. Sison-Young, R. E. Jenkins, Å. Nordling, S. Mkrtchian, B. K. Park, N. R. Kitteringham, C. E. P. Goldring, V. M. Lauschke and M. Ingelman-Sundberg, *Scientific Reports 2016 6:1*, 2016, **6**, 1–13.

70 V. M. Lauschke, D. F. G. Hendriks, C. C. Bell, T. B. Andersson and M. Ingelman-Sundberg, *Chemical Research in Toxicology*, 2016, **29**, 1936–1955.

71 D. F. G. Hendriks, L. F. Puigvert, S. Messner, W. Mortiz and M. Ingelman-Sundberg, *Scientific Reports 2016 6:1*, 2016, **6**, 1–12.

72 M. Štampar, B. Breznik, M. Filipič and B. Žegura, *Cells*, , DOI:10.3390/CELLS9122557.

73 C. Selden, C. W. Spearman, D. Kahn, M. Miller, A. Figaji, E. Erro, J. Bundy, I. Massie, S. A. Chalmers, H. Arendse, A. Gautier, P. Sharratt, B. Fuller and H. Hodgson, *PLoS ONE*, 2013, **8**, 82312.

74 X. L. Guo, K. S. Yang, J. Y. Hyun, W. S. Kim, D. H. Lee, K. E. Min, L. S. Park, K. H. Seo, Y. I. Kim, C. S. Cho and I. K. Kang, *J Biomater Sci Polym Ed*, 2003, **14**, 551–565.

75 F. Pati and D. W. Cho, *Methods in Molecular Biology*, 2017, **1612**, 381–390.

76 I. Matai, G. Kaur, A. Seyedsalehi, A. McClinton and C. T. Laurencin, *Biomaterials*, 2020, **226**, 119536.

77 M. Ruoß, M. Vosough, A. Königsrainer, S. Nadalin, S. Wagner, S. Sajadian, D. Huber, Z. Heydari, S. Ehnert, J. G. Hengstler and A. K. Nussler, *Food and Chemical Toxicology*, 2020, **138**, 111188.

78 M. A. Polidoro, E. Ferrari, S. Marzorati, A. Lleo and M. Rasponi, *Liver International*, 2021, **41**, 1744–1761.

79 D. Bovard, A. Iskandar, K. Luettich, J. Hoeng and M. C. Peitsch, *http://dx.doi.org/10.1177/2397847317726351*, 2017, **1**, 239784731772635.

80 E. Moradi, S. Jalili-Firoozinezhad and M. Solati-Hashjin, *Acta Biomaterialia*, 2020, **116**, 67–83.

81 A. Redaelli and M. Long, *APL Bioengineering*, 2022, **6**, 020401.

82 D. E. Ingber, *Advanced Science*, 2020, **7**, 2002030.

83 S. N. Bhatia and D. E. Ingber, *Nature Biotechnology 2014 32:8*, 2014, **32**, 760–772.

84 M. Piergiovanni, S. B. Leite, R. Corvi and M. Whelan, *Lab on a Chip*, 2021, **21**, 2857–2868.

85 D. van Berlo, E. van de Steeg, H. E. Amirabadi and R. Masereeuw, *Current Opinion in Toxicology*, 2021, **27**, 8–17.

86 P. Akarapipad, K. Kaarj, Y. Liang and J. Y. Yoon, *Annual Review of Analytical Chemistry*, 2021, **14**, 155–183.

87 A. Essaouiba, T. Okitsu, R. Jellali, M. Shinohara, M. Danoy, Y. Tauran, C. Legallais, Y. Sakai and E. Leclerc, *Molecular and Cellular Endocrinology*, 2020, **514**, 110892.

88 M. Malik, Y. Yang, P. Fathi, G. J. Mahler and M. B. Esch, *Frontiers in Cell and Developmental Biology*, 2021, **9**, 2353.

89 N. Picollet-D'hahan, A. Zuchowska, I. Lemeunier and S. le Gac, *Trends in Biotechnology*, 2021, **39**, 788–810.

90 F. Kurth, E. Györvary, S. Heub, D. Ledroit, S. Paoletti, K. Renggli, V. Revol, M. Verhulsel, G. Weder and F. Loizeau, *Organ-on-a-chip: Engineered Microenvironments for Safety and Efficacy Testing*, 2020, 47–130.

91 S. B. Campbell, Q. Wu, J. Yazbeck, C. Liu, S. Okhovatian and M. Radisic, *ACS Biomaterials Science & Engineering*, 2020, **7**, 2880–2899.

92 S. Ahadian, R. Civitarese, D. Bannerman, M. H. Mohammadi, R. Lu, E. Wang, L. Davenport-Huyer, B. Lai, B. Zhang, Y. Zhao, S. Mandla, A. Korolj and M. Radisic, *Advanced Healthcare Materials*, 2018, **7**, 1700506.

93 H. Suzuki, K. Mitsuno, K. Shiroguchi, M. Tsugane, T. Okano, T. Dohi and T. Tsuji, *Lab on a Chip*, 2017, **17**, 647–652.

94 M. W. Toepke and D. J. Beebe, *Lab on a Chip*, 2006, **6**, 1484–1486.

95 C. Ding, X. Chen, Q. Kang and X. Yan, *Frontiers in Bioengineering and Biotechnology*, 2020, **8**, 823.

96 E. Sollier, C. Murray, P. Maoddi and D. di Carlo, *Lab on a Chip*, 2011, **11**, 3752–3765.

97 K. Ren, J. Zhou and H. Wu, *Accounts of Chemical Research*, 2013, **46**, 2396–2406.

98 R. Jellali, P. Paullier, M. J. Fleury and E. Leclerc, *Sensors and Actuators B: Chemical*, 2016, **229**, 396–407.

99 E. Gencturk, S. Mutlu and K. O. Ulgen, *Biomicrofluidics*, 2017, **11**, 051502.

100 C. W. Chang, Y. J. Cheng, M. Tu, Y. H. Chen, C. C. Peng, W. H. Liao and Y. C. Tung, *Lab on a Chip*, 2014, **14**, 3762–3772.

101 M. Tonin, N. Descharmes and R. Houdré, *Lab on a Chip*, 2016, **16**, 465–470.

102 K. Tan, P. Keegan, M. Rogers, M. Lu, J. R. Gosset, J. Charest and S. S. Bale, *Lab on a Chip*, 2019, **19**, 1556–1566.

103 G. Kulsharova, A. Kurmangaliyeva, E. Darbayeva, L. Rojas-Solórzano and G. Toxeitova, *Polymers 2021, Vol. 13, Page 3215*, 2021, **13**, 3215.

104 N. Bhattacharjee, A. Urrios, S. Kang and A. Folch, *Lab on a Chip*, 2016, **16**, 1720–1742.

105 H. G. Yi, H. Lee and D. W. Cho, *Bioengineering*, , DOI:10.3390/bioengineering4010010.

106 J. R. Puryear, J. K. Yoon and Y. T. Kim, *Micromachines 2020, Vol. 11, Page 730*, 2020, **11**, 730.

107 C. W. Tsao, *Micromachines (Basel)*, 2016, 7, 225.

108 A. Waldbaur, H. Rapp, K. Länge and B. E. Rapp, *Analytical Methods*, 2011, 3, 2681–2716.

109 G. Weisgrab, A. Ovsianikov and P. F. Costa, *Advanced Materials Technologies*, 2019, **4**, 1900275.

110 C. M. B. Ho, S. H. Ng, K. H. H. Li and Y. J. Yoon, *Lab on a Chip*, 2015, **15**, 3627–3637.

111 Y. Zhou, *Journal of Biomedical Science 2017 24:1*, 2017, **24**, 1–22.

112 K. Zeilinger, N. Freyer, G. Damm, D. Seehofer and F. Knöspel, *Experimental Biology and Medicine*, 2016, **241**, 1684–1698.

113 M. T. Donato and L. Tolosa, *Differentiation*, 2019, **106**, 15–22.

114 S. R. Khetani, D. R. Berger, K. R. Ballinger, M. D. Davidson, C. Lin and B. R. Ware, *Journal of Laboratory Automation*, 2015, **20**, 216–250.

115 E. L. LeCluyse, E. Alexandre, G. A. Hamilton, C. Viollon-Abadie, D. J. Coon, S. Jolley and L. Richert, *Methods Mol Biol*, 2005, **290**, 207–229.

116 M. Hegde, R. Jindal, A. Bhushan, S. S. Bale, W. J. McCarty, I. Golberg, O. B. Usta and M. L. Yarmush, *Lab on a Chip*, 2014, **14**, 2033–2039.

117 R. Jellali, T. Bricks, S. Jacques, M. J. Fleury, P. Paullier, F. Merlier and E. Leclerc, *Biopharmaceutics & Drug Disposition*, 2016, **37**, 264–275.

118 H. Olson, G. Betton, D. Robinson, K. Thomas, A. Monro, G. Kolaja, P. Lilly, J. Sanders, G. Sipes, W. Bracken, M. Dorato, K. van Deun, P. Smith, B. Berger and A. Heller, *Regulatory Toxicology and Pharmacology*, 2000, **32**, 56–67.

119 A. Burkard, C. Dähn, S. Heinz, A. Zutavern, V. Sonntag-Buck, D. Maltman, S. Przyborski, N. J. Hewitt and J. Braspenning, *https://doi.org/10.3109/00498254.2012.675093*, 2012, **42**, 939–956.

120 S. D. Ramachandran, A. Vivarès, S. Klieber, N. J. Hewitt, B. Muenst, S. Heinz, H. Walles and J. Braspenning, *Pharmacology Research & Perspectives*, 2015, **3**, e00161.

121 L. Tolosa, M. J. Gómez-Lechón, S. López, C. Guzmán, J. v. Castell, M. T. Donato and R. Jover, *Toxicological Sciences*, 2016, **152**, 214–229.

122 M. Donato, R. Jover and M. Gómez-Lechón, *Current Drug Metabolism*, 2013, **14**, 946–968.

123 M. Gomez-Lechon, M. Donato, A. Lahoz and J. Castell, *Current Drug Metabolism*, 2008, **9**, 1–11.

124 L. Kuna, I. Bozic, T. Kizivat, K. Bojanic, M. Mrso, E. Kralj, R. Smolic, G. Y. Wu and M. Smolic, *Current Drug Metabolism*, 2018, **19**, 830–838.

125 J. Deng, W. Wei, Z. Chen, B. Lin, W. Zhao, Y. Luo and X. Zhang, *Micromachines (Basel)*, 2019, **10**, 1–26.

126 M. J. Gómez-Lechón, L. Tolosa, I. Conde and M. T. Donato, *https://doi.org/10.1517/17425255.2014.967680*, 2014, **10**, 1553–1568.

127 J. C. Fernandez-Checa, P. Bagnaninchi, H. Ye, P. Sancho-Bru, J. M. Falcon-Perez, F. Royo, C. Garcia-Ruiz, O. Konu, J. Miranda, O. Lunov, A. Dejneka, A. Elfick, A. McDonald, G. J. Sullivan, G. P. Aithal, M. I. Lucena, R. J. Andrade, B. Fromenty, M. Kranendonk, F. J. Cubero and L. J. Nelson, *Journal of Hepatology*, 2021, **75**, 935–959.

128 M. Coll, L. Perea, R. Boon, S. B. Leite, J. Vallverdú, I. Mannaerts, A. Smout, A. el Taghdouini, D. Blaya, D. Rodrigo-Torres, I. Graupera, B. Aguilar-Bravo, C. Chesne, M. Najimi, E. Sokal, J. J. Lozano, L. A. van Grunsven, C. M. Verfaillie and P. Sancho-Bru, *Cell Stem Cell*, 2018, **23**, 101-113.e7.

129 L. Boeri, L. Izzo, L. Sardelli, M. Tunesi, D. Albani and C. Giordano, *Bioengineering 2019, Vol. 6, Page 91*, 2019, **6**, 91.

130 V. Volarevic, B. S. Markovic, M. Gazdic, A. Volarevic, N. Jovicic, N. Arsenijevic, L. Armstrong, V. Djonov, M. Lako and M. Stojkovic, *International Journal of Medical Sciences*, 2018, 15, 36–45.

131 K. Takahashi, K. Tanabe, M. Ohnuki, M. Narita, T. Ichisaka, K. Tomoda and S. Yamanaka, *Cell*, , DOI:10.1016/j.cell.2007.11.019.

132 P. Karagiannis, K. Takahashi, M. Saito, Y. Yoshida, K. Okita, A. Watanabe, H. Inoue, J. K. Yamashita, M. Todani, M. Nakagawa, M. Osawa, Y. Yashiro, S. Yamanaka and K. Osafune, *Physiological Reviews*, 2019, **99**, 79–114.

133 K. Si-Tayeb, F. K. Noto, M. Nagaoka, J. Li, M. A. Battle, C. Duris, P. E. North, S. Dalton and S. A. Duncan, *Hepatology*, 2010, **51**, 297–305.

134 K. Takayama, M. Inamura, K. Kawabata, K. Katayama, M. Higuchi, K. Tashiro, A. Nonaka, F. Sakurai, T. Hayakawa, M. Kusuda Furue and H. Mizuguchi, *Molecular Therapy*, 2012, **20**, 127–137.

135 B. R. Ware, D. R. Berger and S. R. Khetani, *Toxicological Sciences*, , DOI:10.1093/toxsci/kfv048.

136 A. Gough, A. Soto-Gutierrez, L. Vernetti, M. R. Ebrahimkhani, A. M. Stern and D. L. Taylor, *Nature Reviews Gastroenterology & Hepatology 2020 18:4*, 2020, **18**, 252–268.

137 L. Xu, A. Y. Hui, E. Albanis, M. J. Arthur, S. M. O'Byrne, W. S. Blaner, P. Mukherjee, S. L. Friedman and F. J. Eng, *Gut*, 2005, **54**, 142–151.

138 A. S. Khazali, A. M. Clark and A. Wells, *Stem Cell Reviews and Reports 2017 13:3*, 2017, **13**, 364–380.

139 S. W. Maepa and H. Ndlovu, *Stem Cells*, 2020, **38**, 606–612.

140 Y. Koui, T. Kido, T. Ito, H. Oyama, S. W. Chen, Y. Katou, K. Shirahige and A. Miyajima, *Stem Cell Reports*, 2017, **9**, 490–498.

141 M. Danoy, R. Jellali, Y. Tauran, J. Bruce, M. Leduc, F. Gilard, B. Gakière, B. Scheidecker, T. Kido, A. Miyajima, F. Soncin, Y. Sakai and E. Leclerc, *Differentiation*, 2021, **120**, 28–35.

142 J. Vallverdú, R. A. Martínez García de la Torre, I. Mannaerts, S. Verhulst, A. Smout, M. Coll, S. Ariño, T. Rubio-Tomás, B. Aguilar-Bravo, C. Martínez-Sánchez, D. Blaya, C. M. Verfaillie, L. A. van Grunsven and P. Sancho-Bru, *Nature Protocols 2021 16:5*, 2021, **16**, 2542–2563.

143 F. Tasnim, J. Xing, X. Huang, S. Mo, X. Wei, M. H. Tan and H. Yu, *Biomaterials*, 2019, **192**, 377–391.

144 F. Sampaziotis, M. C. de Brito, P. Madrigal, A. Bertero, K. Saeb-Parsy, F. A. C. Soares, E. Schrumpf, E. Melum, T. H. Karlsen, J. A. Bradley, W. T. H. Gelson, S. Davies, A. Baker, A. Kaser, G. J. Alexander, N. R. F. Hannan and L. Vallier, *Nature Biotechnology 2015 33:8*, 2015, **33**, 845–852.

145 T. M. de Assuncao, Y. Sun, N. Jalan-Sakrikar, M. C. Drinane, B. Q. Huang, Y. Li, J. I. Davila, R. Wang, S. P. O'Hara, G. A. Lomberk, R. A. Urrutia, Y. Ikeda and R. C. Huebert, *Laboratory Investigation 2015 95:6*, 2015, **95**, 684–696.

146 T. Tricot, C. M. Verfaillie and M. Kumar, *Cells 2022, Vol. 11, Page 442*, 2022, **11**, 442.

147 S. Kidambi, L. Sheng, M. L. Yarmush, M. Toner, I. Lee and C. Chan, *Macromolecular Bioscience*, 2007, **7**, 344–353.

148 J. W. Allen and S. N. Bhatia, *Biotechnology and Bioengineering*, 2003, **82**, 253–262.

149 J. W. Allen, S. R. Khetani and S. N. Bhatia, *Toxicological Sciences*, 2005, **84**, 110–119.

150 C. A. Schoenenberger, A. Zuk, G. M. Zinkl, D. Kendall and K. S. Matlin, *Journal of Cell Science*, 1994, **107**, 527–541.

151 S. Ng, R. Han, S. Chang, J. Ni, W. Hunziker, A. B. Goryachev, S. H. Ong and H. Yu, *https://home.liebertpub.com/ten*, 2006, **12**, 2181–2191.

152 L. Xia, S. Ng, R. Han, X. Tuo, G. Xiao, H. L. Leo, T. Cheng and H. Yu, *Biomaterials*, 2009, **30**, 5927–5936.

153 H. W. Lee, Y. M. Kook, H. J. Lee, H. Park and W. G. Koh, *RSC Advances*, 2014, **4**, 61005–61011.

154 L. D. Ma, Y. T. Wang, J. R. Wang, J. L. Wu, X. S. Meng, P. Hu, X. Mu, Q. L. Liang and G. A. Luo, *Lab on a Chip*, 2018, **18**, 2547–2562.

155 Y. S. Weng, S. F. Chang, M. C. Shih, S. H. Tseng and C. H. Lai, *Advanced Materials*, 2017, **29**, 1701545.

156 X. Cui, Y. Hartanto and H. Zhang, *Journal of The Royal Society Interface*, , DOI:10.1098/RSIF.2016.0877.

157 Y. Fang and R. M. Eglen, *Slas Discovery*, 2017, **22**, 456.

158 Y. C. Toh, T. C. Lim, D. Tai, G. Xiao, D. van Noort and H. Yu, *Lab on a Chip*, 2009, **9**, 2026–2035.

159 L. Boulais, R. Jellali, U. Pereira, E. Leclerc, S. A. Bencherif and C. Legallais, *ACS Applied Bio Materials*, 2021, **4**, 5617–5626.

160 S. Massa, M. A. Sakr, J. Seo, P. Bandaru, A. Arneri, S. Bersini, E. Zare-Eelanjegh, E. Jalilian, B. H. Cha, S. Antona, A. Enrico, Y. Gao, S. Hassan, J. P. Acevedo, M. R. Dokmeci, Y. S. Zhang, A. Khademhosseini and S. R. Shin, *Biomicrofluidics*, 2017, **11**, 044109.

161 F. Yu and D. Choudhury, *Drug Discovery Today*, 2019, **24**, 1248–1257.

162 H. Lee and D. W. Cho, *Lab on a Chip*, 2016, **16**, 2618–2625.

163 J. E. Snyder, Q. Hamid, C. Wang, R. Chang, K. Emami, H. Wu and W. Sun, *Biofabrication*, 2011, **3**, 034112.

164 N. S. Bhise, V. Manoharan, S. Massa, A. Tamayol, M. Ghaderi, M. Miscuglio, Q. Lang, Y. S. Zhang, S. R. Shin, G. Calzone, N. Annabi, T. D. Shupe, C. E. Bishop, A. Atala, M. R. Dokmeci and A. Khademhosseini, *Biofabrication*, , DOI:10.1088/1758-5090/8/1/014101.

165 S. Knowlton and S. Tasoglu, *Trends in Biotechnology*, 2016, **34**, 681–682.

166 V. Palacio-Castañeda, N. Velthuijs, S. le Gac and W. P. R. Verdurmen, *Lab on a Chip*, 2022, **22**, 1068–1092.

167 K. Funamoto, I. K. Zervantonakis, Y. Liu, C. J. Ochs, C. Kim and R. D. Kamm, *Lab on a Chip*, 2012, **12**, 4855–4863.

168 J. J. F. Sleeboom, J. M. J. den Toonder, C. M. Sahlgren, J. J. F. Sleeboom@tue, J. J. F. S. Nl, J. M. J. D. Toonder@tue and J. M. J. D. T. Nl, *International Journal of Molecular Sciences 2018, Vol. 19, Page 3047*, 2018, **19**, 3047.

169 F. T. Lee-Montiel, S. M. George, A. H. Gough, A. D. Sharma, J. Wu, R. DeBiasio, L. A. Vernetti and D. L. Taylor, *Experimental Biology and Medicine*, 2017, **242**, 1617–1632.

170 W. J. McCarty, O. B. Usta and M. L. Yarmush, *Scientific Reports 2016 6:1*, 2016, **6**, 1–10.

171 J. H. Lee, K. L. Ho and S. K. Fan, *Journal of Biomedical Science*, 2019, **26**, 1–10.

172 M. Hegde, R. Jindal, A. Bhushan, S. S. Bale, W. J. McCarty, I. Golberg, O. B. Usta and M. L. Yarmush, *Lab on a Chip*, 2014, **14**, 2033–2039.

173 L. Prodanov, R. Jindal, S. S. Bale, M. Hegde, W. J. Mccarty, I. Golberg, A. Bhushan, M. L. Yarmush and O. B. Usta, *Biotechnol Bioeng*, 2016, **113**, 241–246.

174 Y. Du, N. Li, H. Yang, C. Luo, Y. Gong, C. Tong, Y. Gao, S. Lü and M. Long, *Lab on a Chip*, 2017, **17**, 782–794.

175 F. Cheng, W. Li, Y. Zhou, J. Shen, Z. Wu, G. Liu, P. W. Lee and Y. Tang, *Journal of Chemical Information and Modeling*, 2012, **52**, 3099–3105.

176 E. F. A. Brandon, C. D. Raap, I. Meijerman, J. H. Beijnen and J. H. M. Schellens, *Toxicology and Applied Pharmacology*, 2003, **189**, 233–246.

177 A. Sivaraman, J. Leach, S. Townsend, T. Iida, B. Hogan, D. Stolz, R. Fry, L. Samson, S. Tannenbaum and L. Griffith, *Current Drug Metabolism*, 2005, **6**, 569–591.

178 A. R. Baudy, M. A. Otieno, P. Hewitt, J. Gan, A. Roth, D. Keller, R. Sura, T. R. van Vleet and W. R. Proctor, *Lab on a Chip*, 2020, **20**, 215–225.

179 B. Fromenty and D. Pessayre, *Pharmacology & Therapeutics*, 1995, **67**, 101–154.

180 M. Leist, B. Single, A. F. Castoldi, S. Kühnle and P. Nicotera, *Journal of Experimental Medicine*, 1997, **185**, 1481–1486.

181 B. H. Lee, W.-J. Koh, M. S. Choi, G. Y. Suh, M. P. Chung, H. Kim and O. J. Kwon, *Chest*, 2005, **127**, 1304–1311.

182 L. B. Seeff, B. A. Cuccherini, H. J. Zimmerman, E. Adler and S. B. Benjamin, *Annals of Internal Medicine*, 1986, **104**, 399–404.

183 E. S. Zafrani, K. G. Ishak and C. Rudzki, *Cholestatic and Hepatocellular Injury Associated with Erythromycin Esters Report of Nine Cases RESULTS I. Clinical Findings*, 1979, vol. 24.

184 L. C. Snouber, A. Bunescu, M. Naudot, C. Legallais, C. Brochot, M. E. Dumas, B. Elena-Herrmann and E. Leclerc, *Toxicological Sciences*, 2013, **132**, 8–20.

185 J. M. Prot, A. S. Briffaut, F. Letourneur, P. Chafey, F. Merlier, Y. Grandvalet, C. Legallais and E. Leclerc, *PLOS ONE*, 2011, **6**, e21268.

186 A. Zuchowska, K. Kwapiszewska, M. Chudy, A. Dybko and Z. Brzozka, *ELECTROPHORESIS*, 2017, **38**, 1206–1216.

187 F. Yu, R. Deng, W. Hao Tong, L. Huan, N. Chan Way, A. Islambadhan, C. Iliescu and H. Yu, *Scientific Reports 2017 7:1*, 2017, **7**, 1–16.

188 K. J. Jang, M. A. Otieno, J. Ronxhi, H. K. Lim, L. Ewart, K. R. Kodella, D. B. Petropolis, G. Kulkarni, J. E. Rubins, D. Conegliano, J. Nawroth, D. Simic, W. Lam, M. Singer, E. Barale, B. Singh, M. Sonee, A. J. Streeter, C. Manthey, B. Jones, A. Srivastava, L. C. Andersson, D. Williams, H. Park, R. Barrile, J. Sliz, A. Herland, S. Haney, K. Karalis, D. E. Ingber and G. A. Hamilton, *Science Translational Medicine*, , DOI:10.1126/SCITRANSLMED.AAX5516/SUPPL_FILE/AAX5516_SM.PDF.

189 S. Mostafalou and M. Abdollahi, *Archives of Toxicology 2016 91:2*, 2016, **91**, 549–599.

190 Life Sciences | Special issue on Environmental Toxicants and Chronic Diseases | ScienceDirect.com by Elsevier, https://www.sciencedirect.com/journal/life-sciences/special-issue/10735TD0LKX, (accessed February 8, 2022).

191 R. Jellali, F. Gilard, V. Pandolfi, A. Legendre, M. J. Fleury, P. Paullier, C. Legallais and E. Leclerc, *Journal of Applied Toxicology*, 2018, **38**, 1121–1134.

192 E. Diamanti-Kandarakis, J. P. Bourguignon, L. C. Giudice, R. Hauser, G. S. Prins, A. M. Soto, R. T. Zoeller and A. C. Gore, *Endocrine Reviews*, 2009, **30**, 293.

193 Á. Mérida-Ortega, S. J. Rothenberg, L. Torres-Sánchez, L. Schnaas, C. Hernández-Alcaraz, M. E. Cebrián, R. M. García-Hernández, R. Ogaz-González and L. López-Carrillo, *Environ Health*, , DOI:10.1186/S12940-019-0456-8.

194 L. M. Rodríguez-Alcalá, C. Sá, L. L. Pimentel, D. Pestana, D. Teixeira, A. Faria, C. Calhau and A. Gomes, *J Agric Food Chem*, 2015, **63**, 9341–9348.

195 R. Jellali, S. Jacques, A. Essaouiba, F. Gilard, F. Letourneur, B. Gakière, C. Legallais and E. Leclerc, *Food and Chemical Toxicology*, 2021, **152**, 112155.

196 R. Jellali, P. Zeller, F. Gilard, A. Legendre, M. J. Fleury, S. Jacques, G. Tcherkez and E. Leclerc, *Environmental Toxicology and Pharmacology*, 2018, **59**, 1–12.

197 K. Radad, M. Al-Shraim, A. Al-Emam, F. Wang, B. Kranner, W. D. Rausch and R. Moldzio, *Folia Neuropathol*, 2019, **57**, 317–326.

198 N. Katila, S. Bhurtel, P. H. Park and D. Y. Choi, *Neurochem Int*, , DOI:10.1016/J.NEUINT.2021.105120.

199 D. Bavli, S. Prill, E. Ezra, G. Levy, M. Cohen, M. Vinken, J. Vanfleteren, M. Jaeger and Y. Nahmias, *Proc Natl Acad Sci U S A*, 2016, **113**, E2231–E2240.

200 N. Singh, G. J. S. Jenkins, R. Asadi and S. H. Doak, *Nano Reviews*, 2010, **1**, 5358.

201 T. Vangijzegem, D. Stanicki and S. Laurent, *Expert Opin Drug Deliv*, 2019, **16**, 69–78.

202 L. Li, K. Gokduman, A. Gokaltun, M. L. Yarmush and O. B. Usta, *Nanomedicine*, 2019, **14**, 2209–2226.

203 T. Jiang, H. Guo, Y. N. Xia, Y. Liu, D. Chen, G. Pang, Y. Feng, H. Yu, Y. Wu, S. Zhang, Y. Wang, Y. Wang, H. Wen and L. W. Zhang, *Nanomedicine (Lond)*, 2021, **16**, 1487–1504.

204 J. Lee, B. Choi, D. Y. No, G. Lee, S. R. Lee, H. Oh and S. H. Lee, *Integrative Biology (United Kingdom)*, 2016, **8**, 302–308.

205 J. Deng, Y. Cong, X. Han, W. Wei, Y. Lu, T. Liu, W. Zhao, B. Lin, Y. Luo and X. Zhang, *Biomicrofluidics*, 2020, **14**, 64107.

206 A. Schepers, C. Li, A. Chhabra, B. T. Seney and S. Bhatia, *Lab Chip*, 2016, **16**, 2644–2653.

207 Y. bo Zheng, L. dong Ma, J. lin Wu, Y. ming Wang, X. sheng Meng, P. Hu, Q. lin Liang, Y. yuan Xie and G. an Luo, *Talanta*, 2022, **241**, 123262.

208 L. Li, K. Gokduman, A. Gokaltun, M. L. Yarmush and O. B. Usta, *Nanomedicine (Lond)*, 2019, **14**, 2209–2226.

209 J. C. Nawroth, D. B. Petropolis, D. v. Manatakis, T. I. Maulana, G. Burchett, K. Schlünder, A. Witt, A. Shukla, K. Kodella, J. Ronxhi, G. Kulkarni, G. Hamilton, E. Seki, S. Lu and K. C. Karalis, *Cell Reports*, , DOI:10.1016/j.celrep.2021.109393.

210 J. Theobald, A. Ghanem, P. Wallisch, A. A. Banaeiyan, M. A. Andrade-Navarro, K. Taškova, M. Haltmeier, A. Kurtz, H. Becker, S. Reuter, R. Mrowka, X. Cheng and S. Wölfl, *ACS Biomaterials Science and Engineering*, 2018, **4**, 78–89.

211 T. M. Marin, N. de Carvalho Indolfo, S. A. Rocco, F. L. Basei, M. de Carvalho, K. de Almeida Gonçalves and E. Pagani, *Chemico-Biological Interactions*, 2019, **299**, 59–76.

212 M. B. Esch, G. J. Mahler, T. Stokol and M. L. Shuler, *Lab on a Chip*, 2014, **14**, 3081–3092.

213 D. Bovard, A. Sandoz, K. Luettich, S. Frentzel, A. Iskandar, D. Marescotti, K. Trivedi, E. Guedj, Q. Dutertre, M. C. Peitsch and J. Hoeng, *Lab on a Chip*, 2018, **18**, 3814–3829.

214 K. Schimek, S. Frentzel, K. Luettich, D. Bovard, I. Rütschle, L. Boden, F. Rambo, H. Erfurth, E. M. Dehne, A. Winter, U. Marx and J. Hoeng, *Scientific Reports 2020 10:1*, 2020, **10**, 1–13.

215 K. Viravaidya, A. Sin and M. L. Shuler, *Biotechnology Progress*, 2004, **20**, 316–323.

216 M. B. Esch, T. L. King and M. L. Shuler, *Annual Review of Biomedical Engineering*, 2011, **13**, 55–72.

217 E. M. Materne, A. P. Ramme, A. P. Terrasso, M. Serra, P. M. Alves, C. Brito, D. A. Sakharov, A. G. Tonevitsky, R. Lauster and U. Marx, *Journal of Biotechnology*, 2015, **205**, 36–46.

218 Z. Li, D. Li, Y. Guo, Y. Wang and W. Su, *Biotechnology Letters*, 2021, **43**, 383–392.

219 P. Soltantabar, E. L. Calubaquib, E. Mostafavi, A. Ghazavi and M. C. Stefan, *Organs-on-a-Chip*, 2021, **3**, 100008.

220 C. P. Pires De Mello, C. Carmona-Moran, C. W. McAleer, J. Perez, E. A. Coln, C. J. Long, C. Oleaga, A. Riu, R. Note, S. Teissier, J. Langer and J. J. Hickman, *Lab on a Chip*, 2020, **20**, 749–759.

221 L. Choucha-Snouber, C. Aninat, L. Grsicom, G. Madalinski, C. Brochot, P. E. Poleni, F. Razan, C. G. Guillouzo, C. Legallais, A. Corlu and E. Leclerc, *Biotechnol Bioeng*, 2013, **110**, 597–608.

222 I. M. Gonçalves, R. O. Rodrigues, A. S. Moita, T. Hori, H. Kaji, R. A. Lima and G. Minas, *Bioprinting*, 2022, **26**, e00202.

223 N. Beißner, S. Reichl and T. Lorenz, *Microsystems for Pharmatechnology: Manipulation of Fluids, Particles, Droplets, and Cells*, 2016, 299–339.

224 C. Ma, Y. Peng, H. Li and W. Chen, *Trends in Pharmacological Sciences*, 2021, **42**, 119–133.

225 T. Kanamori, S. Sugiura and Y. Sakai, *Drug Metabolism and Pharmacokinetics*, 2018, **33**, 40–42.

Fig.1. Liver anatomy and schematic representation of hepatic acinus and zonation in hepatic sinusoid (reproduced with permission from Deng et al., 2019 and Ma et al., 2018).**Fig.2.** Current liver experimental models for toxicity studies. The schematic representation of in vitro models highlights the throughput and physiological relevance of each model (reproduced with permission from Moradi et al., 2020).

Fig.3. A summary of advantages and limitations of the potential cell sources of hepatocytes for in vitro liver OoC models.

Fig.4. Examples of liver OoC platforms with different approaches. (A) laminar-flow perfusion bioreactor for sandwich culture of monolayer of rat hepatocytes (reproduced with permission from Xia et al., 2009); (B) biomimetic liver-on-a-chip platform with V-shape microwells (3D-LOC) allowing HepG2/C3A spheroids formation and long-term culture (reproduced with permission from Ma et al., 2018).

Fig.5. Examples of liver OoC platforms with different approaches. (A) 3D vascularized liver OoC model created with HepG2/C3A cells encapsulated in a gelatin methacryloyl hydrogel and HUVECs cells into a central microchannel (reproduced with permission from Massa et al., 2017); (B) microfluidic liver-on-a-chip model with direct bioprinting approach for the formation of 3D hepatic cell line (HepG2/C3A) spheroids (reproduced with permission from Bhise et al., 2016).

Fig.6. Liver-on-a-chip models for drug toxicity assessment. (A) liver OoC microfluidic system integrating U-shaped designs for HepG2/C3A 3D spheroids formation and culture. The device enables long-term toxicity study of anticancer drug 5-fluorouracil with simple and quick analysis (reproduced with permission from Zuchowska et al., 2017); (B) perfusion-incubator-liver-chip (PIC) for 3D culture of rat hepatocytes. The PIC integrates heater and CO_2 system supply, and used for study of acute and chronic toxicity of APAP and diclofenac (reproduced with permission from Yu et al., 2017).

Fig.7. Liver-on-a-chip models for chemical toxicity assessment. (A) PDMS biochip and platform for 12 biochip parallelization coupled to omics analysis for pesticides (permethrin and DDT) toxicity assessment on rat hepatocytes (reproduced with permission from Jellali et al. 2021); (B) 3D liver-on-chip with primary rat hepatocytes for study of short- and long-term toxicity of superparamagnetic iron oxide nanoparticles (SPION, reproduced with permission from Li et al., 2019).

Fig.8. Multi-organ platforms integrating liver OoC for toxicity studies. (A) liver-lung OoC platform to investigate organ crosstalk and assess the toxicity of inhaled substances, example of aflatoxin B1 (reproduced with permission from Schimek et al., 2020); (B) liver-heart-on-chip device to study the cardiotoxicity induced by doxorubicin and its metabolite (Doxorubicinol) produced by liver compartment (HepG2/C3A cell line, reproduced with permission from Soltantabar et al., 2021).

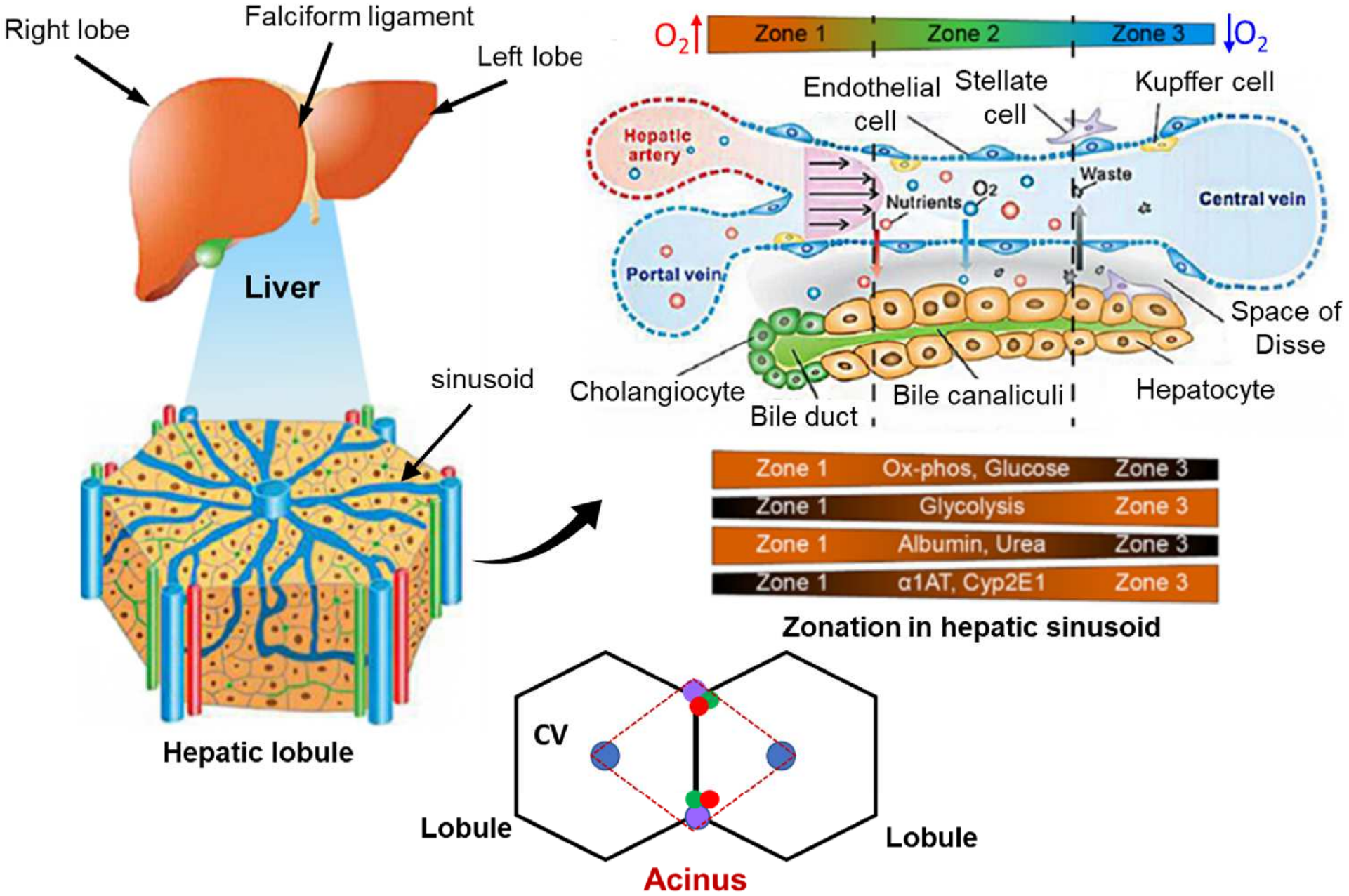
Right lobe
Falciform ligament
Left lobe
Liver
sinusoid
Hepatic lobule
O_2
Zone 1
Zone 2
Zone 3
O_2
Endothelial cell
Stellate cell
Kupffer cell
Hepatic artery
Waste
Nutrients
O_2
Central vein
Portal vein
Space of Disse
Cholangiocyte
Bile duct
Bile canaliculi
Hepatocyte
Zone 1 Ox-phos, Glucose Zone 3
Zone 1 Glycolysis Zone 3
Zone 1 Albumin, Urea Zone 3
Zone 1 α1AT, Cyp2E1 Zone 3
Zonation in hepatic sinusoid
CV
Lobule
Lobule
Acinus

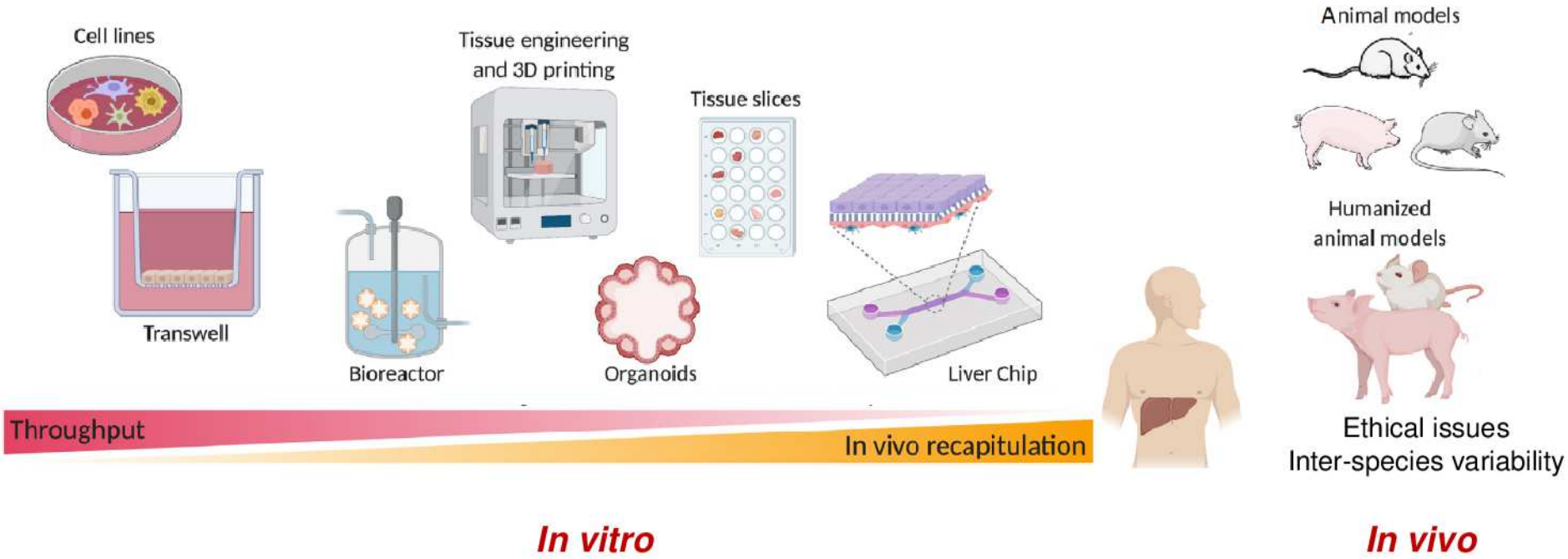
Cell lines
Transwell
Bioreactor
Tissue engineering
and 3D printing
Organoids
Tissue slices
Liver Chip
Animal models
Humanized
animal models
Throughput
In vivo recapitulation
Ethical issues
Inter-species variability
In vitro
In vivo

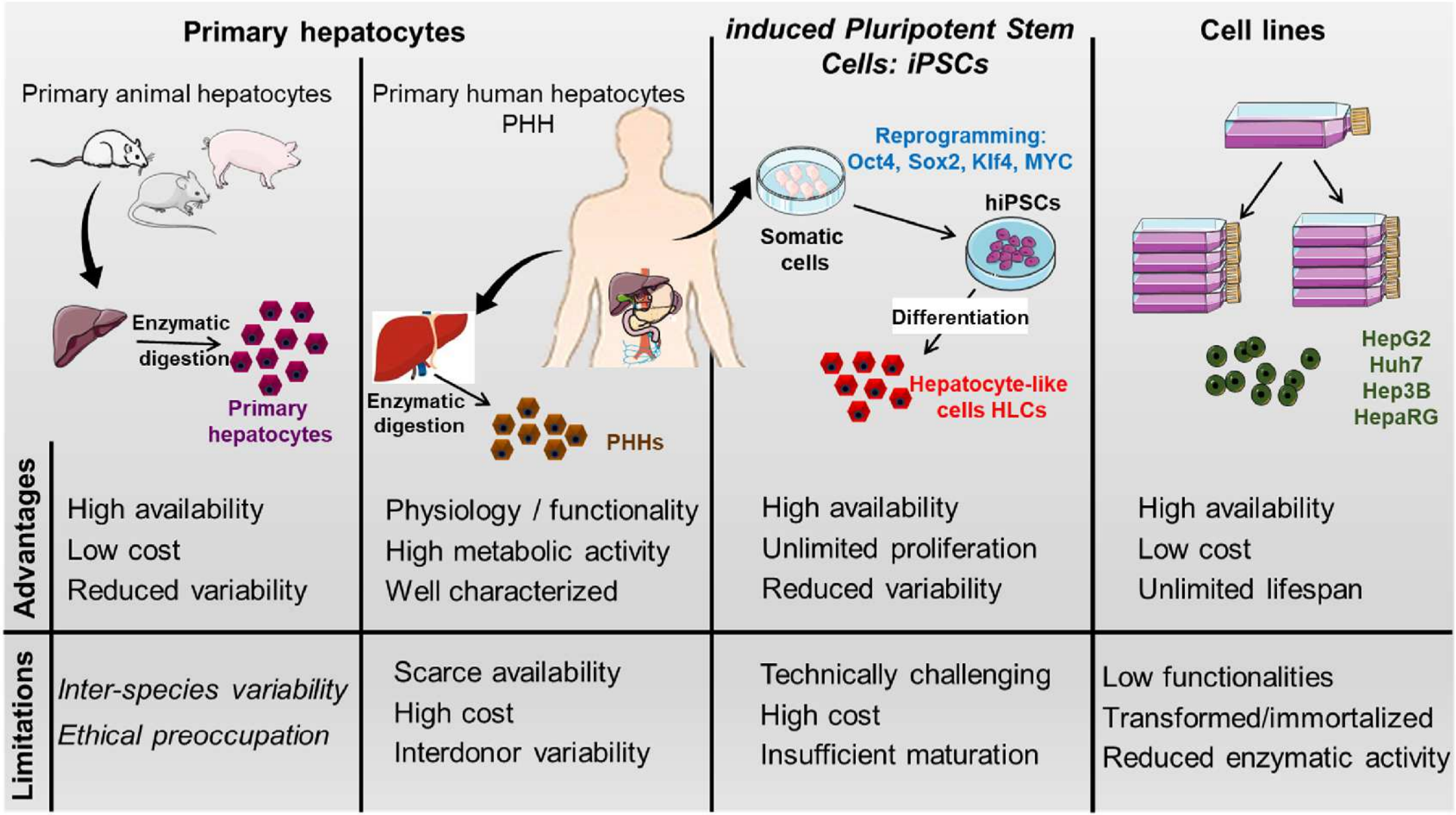
Primary hepatocytes
induced Pluripotent Stem Cells: iPSCs
Cell lines
Primary animal hepatocytes
Primary human hepatocytes PHH
Enzymatic digestion
Primary hepatocytes
Enzymatic digestion
PHHs
Reprogramming: Oct4, Sox2, Klf4, MYC
Somatic cells
hiPSCs
Differentiation
Hepatocyte-like cells HLCs
HepG2
Huh7
Hep3B
HepaRG
Advantages
High availability
Low cost
Reduced variability
Physiology / functionality
High metabolic activity
Well characterized
High availability
Unlimited proliferation
Reduced variability
High availability
Low cost
Unlimited lifespan
Limitations
Inter-species variability
Ethical preoccupation
Scarce availability
High cost
Interdonor variability
Technically challenging
High cost
Insufficient maturation
Low functionalities
Transformed/immortalized
Reduced enzymatic activity

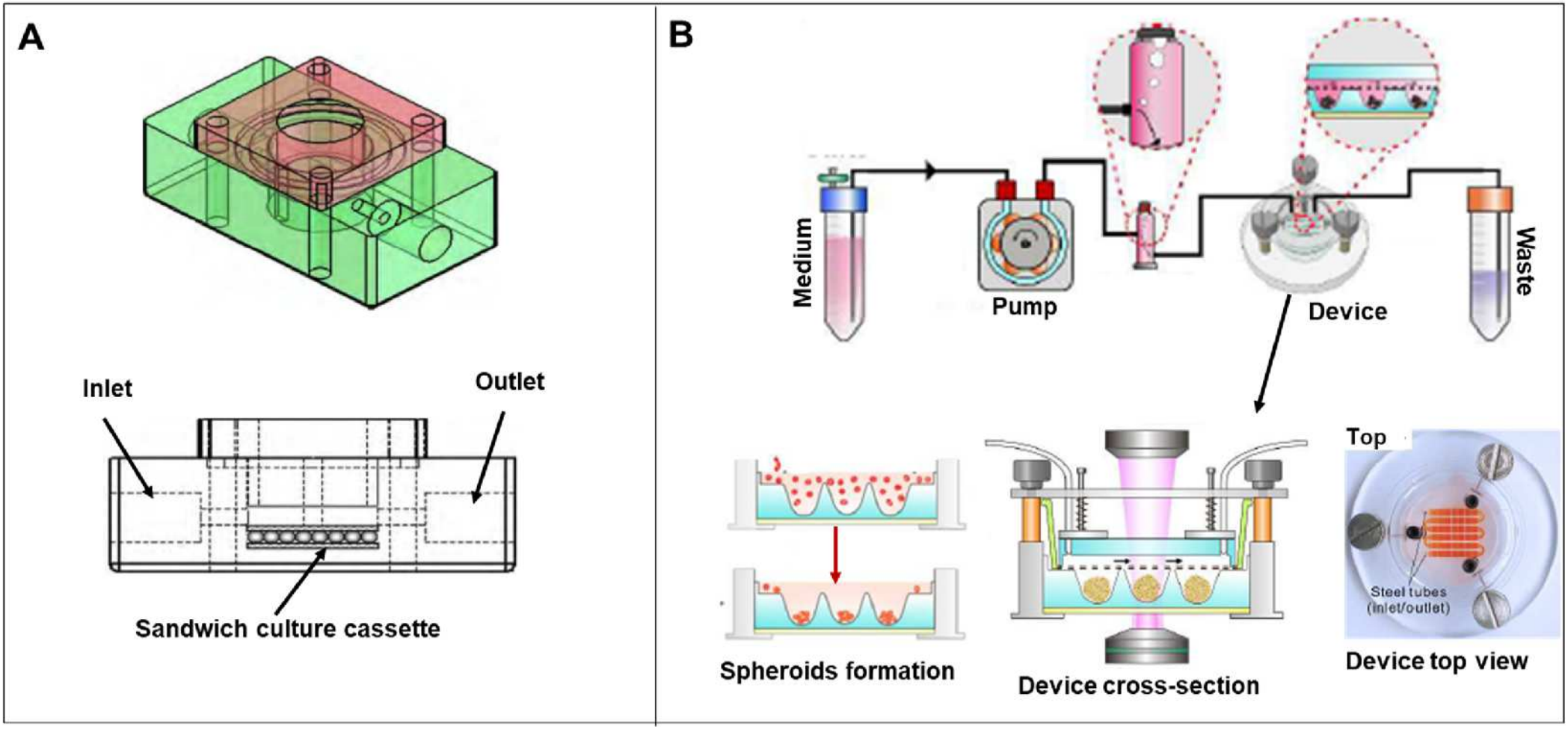
A
Inlet
Outlet
Sandwich culture cassette
B
Medium
Pump
Device
Waste
Spheroids formation
Device cross-section
Top
Steel tubes
(inlet/outlet)
Device top view

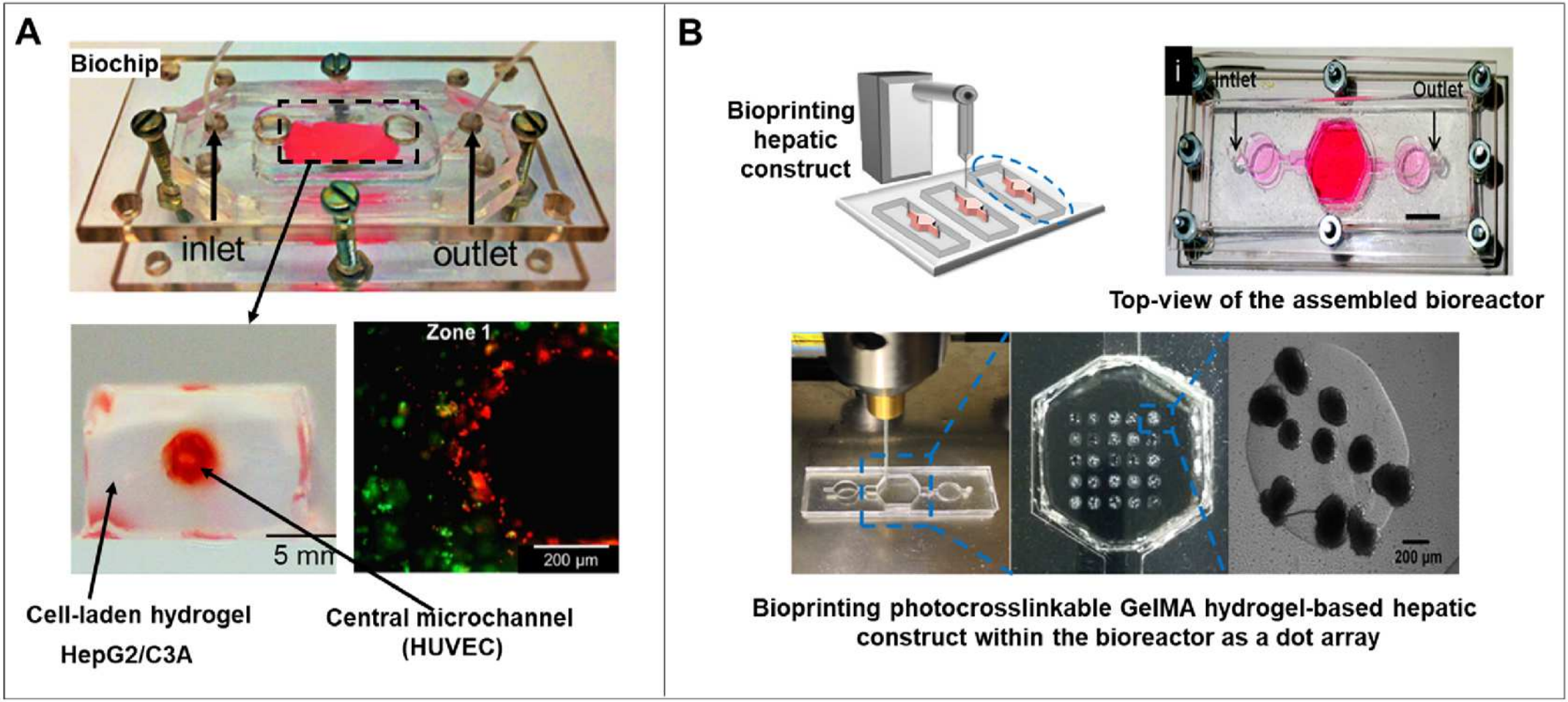
A
Biochip
inlet
outlet
5 mm
Zone 1
200 μm
Cell-laden hydrogel
HepG2/C3A
Central microchannel
(HUVEC)
B
Bioprinting
hepatic
construct
i
Intlet
Outlet
Top-view of the assembled bioreactor
200 μm
Bioprinting photocrosslinkable GelMA hydrogel-based hepatic
construct within the bioreactor as a dot array

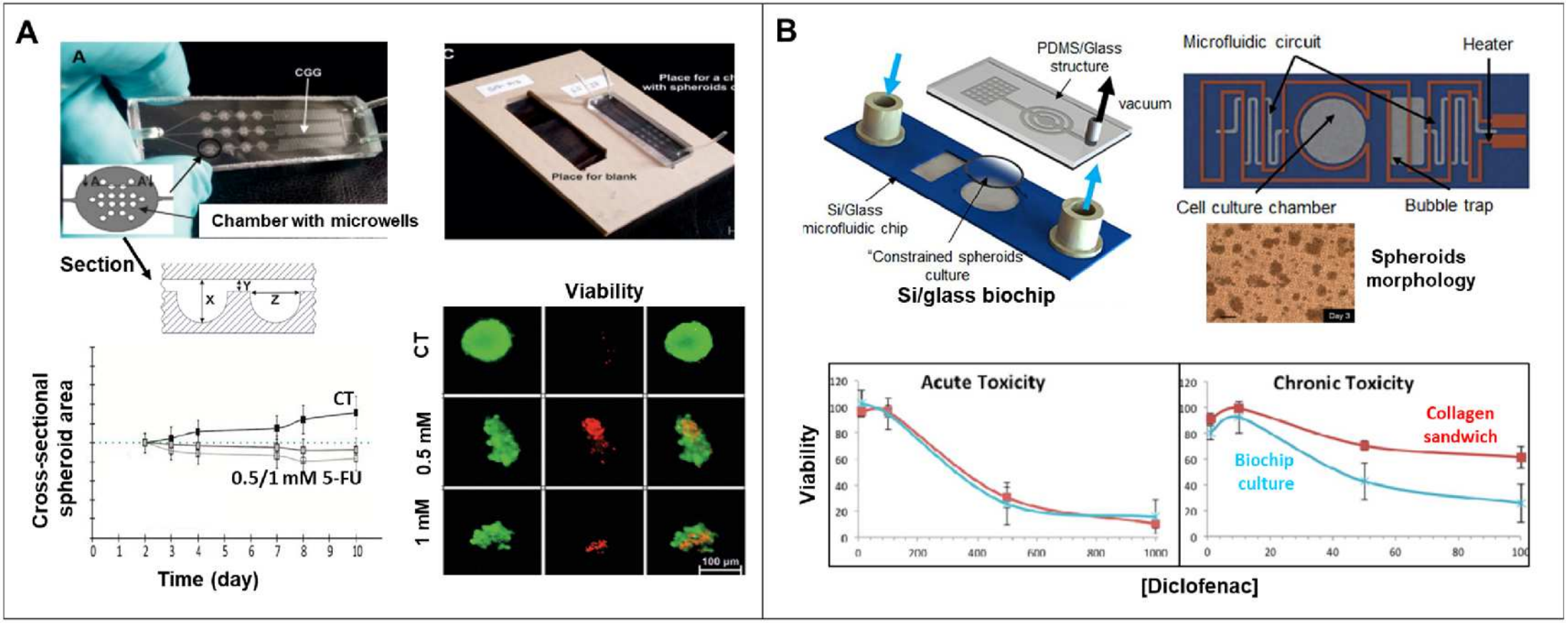
A
CGG
Chamber with microwells
Section
X
Y
Z
Cross-sectional spheroid area
CT
0.5/1 mM 5-FU
0 1 2 3 4 5 6 7 8 9 10
Time (day)
Place for blank
Viability
CT
0.5 mM
1 mM
100 µm
B
PDMS/Glass structure
vacuum
Si/Glass microfluidic chip
"Constrained spheroids culture
Si/glass biochip
Microfluidic circuit
Heater
Cell culture chamber
Bubble trap
Spheroids morphology
Acute Toxicity
Chronic Toxicity
Collagen sandwich
Biochip culture
Viability
[Diclofenac]

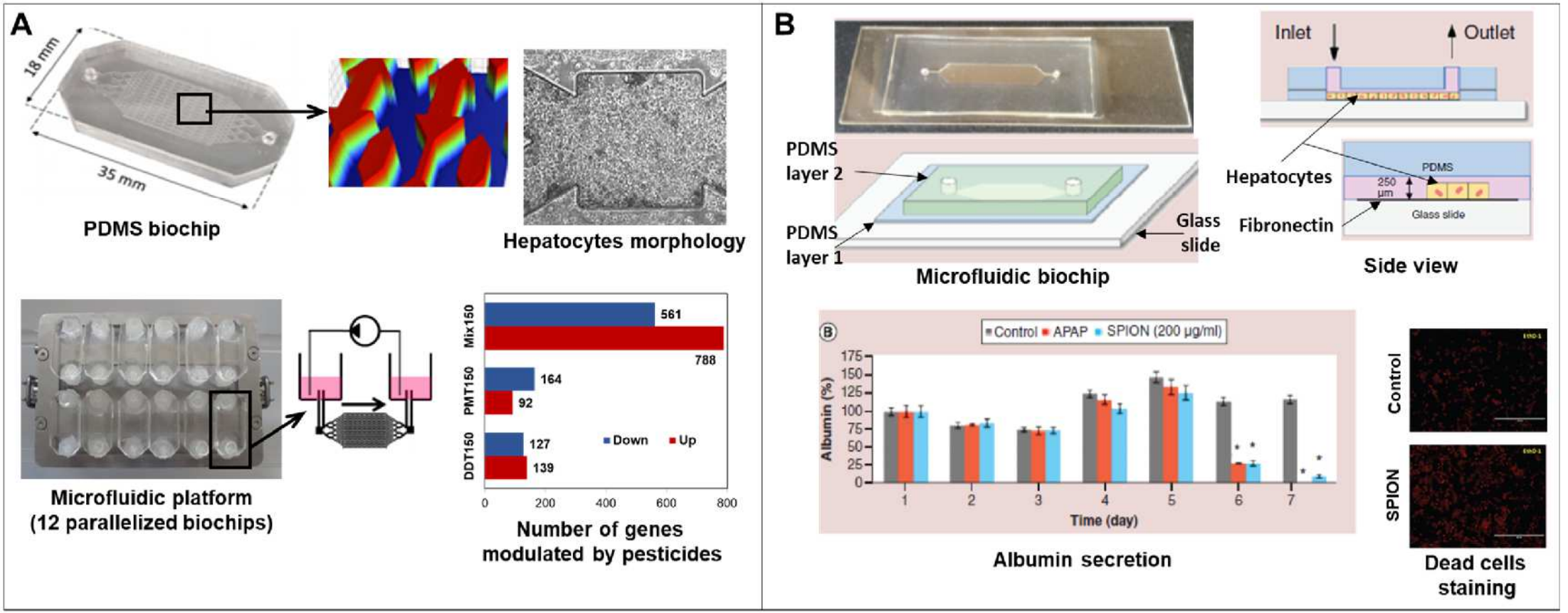
A
18 mm
35 mm
PDMS biochip
Hepatocytes morphology
Microfluidic platform
(12 parallelized biochips)
Mix150
PMT150
DDT150
561
788
164
92
127
139
Down
Up
0
200
400
600
800
Number of genes
modulated by pesticides
B
PDMS
layer 2
PDMS
layer 1
Glass
slide
Microfluidic biochip
Inlet
Outlet
Hepatocytes
Fibronectin
PDMS
250
µm
Glass slide
Side view
Control
APAP
SPION (200 µg/ml)
Albumin (%)
Time (day)
Albumin secretion
Control
SPION
Dead cells
staining

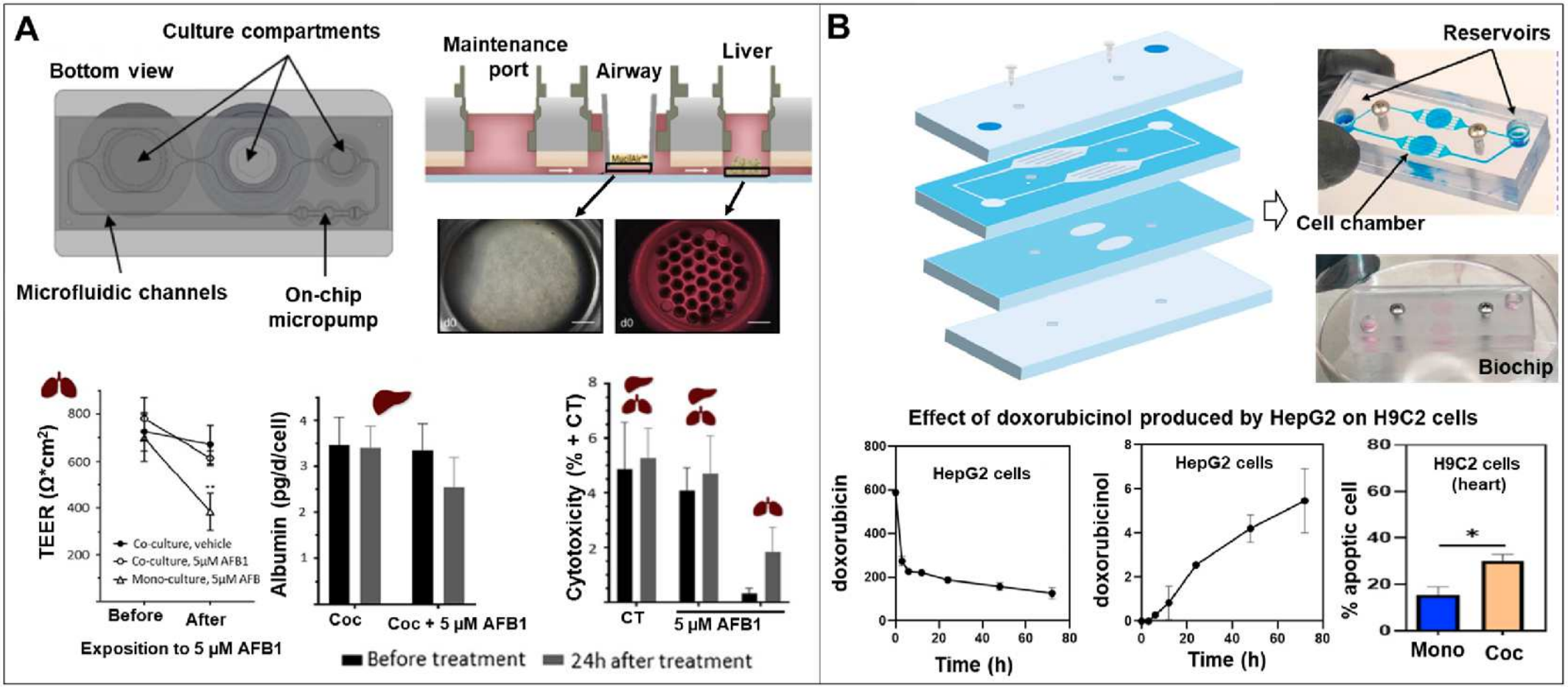
A
Culture compartments
Bottom view
Microfluidic channels
On-chip micropump
Maintenance port
Airway
Liver
TEER (Ω*cm²)
Co-culture, vehicle
Co-culture, 5µM AFB1
Mono-culture, 5µM AFB
Before
After
Exposition to 5 µM AFB1
Albumin (pg/d/cell)
Coc
Coc + 5 µM AFB1
Cytotoxicity (% + CT)
CT
5 µM AFB1
Before treatment
24h after treatment
B
Reservoirs
Cell chamber
Biochip
Effect of doxorubicinol produced by HepG2 on H9C2 cells
doxorubicin
HepG2 cells
Time (h)
doxorubicinol
HepG2 cells
Time (h)
% apoptic cell
H9C2 cells (heart)
Mono
Coc

Table 1. Overview of main liver OoC models used for drug and chemical toxicity studies

	Cell model	Cell organizations/configuration	Drugs / Toxicans	Assays	Outcomes	Ref
Drug toxicity	Primary Rat hepatocytes Fibroblasts: J2-3T3 cell line	2D planar culture	Acetaminophen	Viability, O_2 distribution, CYP3B and CYP3A production	Recreation of the liver zonation Model adapted for the investigation of the spatial and temporal dynamics of hepatotoxicity	149
	HepG2 cell line	3D spheroids (bioprinted in GelMa)	Acetaminophen	Viability, bile canalicular development, albumin, A1AT expression, transferrin, ceruloplasmin	Maintenance of the hepatic functions for 30 days of culture Hepatotoxicity observed in the developed model correlated with the in vivo results	164
	HepG2 cell line	3D spheroids (U-shape wells)	5-fluorouracil	Cross-sectional spheroids area, viability	Model for long-term 3D spheroids culture Simple and quick analysis Correlation between the spheroids size and the development of a resistance to anti-cancer drug	186
	HepG2 cell line	2D (patterned biochip)	Flutamide Hydroxyflutamide	Proliferation, viability metabolic profiling	Demonstration of the potential of metabolomic-on-chip approach for predictive toxicology Correlation between the flutamide exposure and the mitochondrial disruption Extraction of the toxic metabolic signature of flutamide	184
	HepG2 cell line	2D (patterned biochip)	Acetaminophen (APAP)	Proliferation, albumin, APAP metabolism, proteomic and transcriptomic analysis	Enhanced drug metabolism pathways compared to Petri dishes Extraction of the toxic metabolic signature of APAP Toxic metabolic signature similar to in vivo condition	185

	Primary human hepatocytes & dog & rat Co-cultured with LSEC, Kupffer and stellate cells	3D in Matrigel	Bosentan Acetaminophen	Viability, total glutathione, total ATP, albimin secretion, cytokines, gene expression CYP450 enzyme activity, AST, ALT and GDH	Creation of species-specific liver-chip models for drug toxicity assays Highlight of the potential of the model for the relevant detection of species-specific toxicity	188
	Primary rat hepatocytes	3D spheroids (agregated using PET-PAA-AHG and glass-PEG-AHG wells)	Diclofenac Acetaminophen	Viability, urea and albumin secretion, CYP1A2, CYP2B1/2 and CYP3A2 expression	Successfully maintained spheroids functions for 2-3 weeks Model supported repeated chronic and sub-acute drug tests The model integrated a heater, a temperature controller and active debubbler on chip	187
	HepG2 cell line Co-cultured with HUVEC	3D spheroids in GelMa	Acetaminophen	Viability, cellular metabolic activity	Integration of vascularization into the liver model for toxicity study Recreation of the endothelial barrier which delayed the passage of drugs Development of a model that recreate a more relevant in vivo drug response	160
	HepG2 cell line Endothelial cells: HUVEC Stellate cells: LX-2 Monocytes: U937 cell line	2D using materixgel	Acetaminophen	Viability, albumin and urea secretion, cytochrome P450 enzyme activities	Integration of the four hepatic cells layer in the liver-chip Maintenance of cell viability above 70% at day 15 Construction of a dose-and time-dependant APAP-induced disease model	205
	Primary human hepatocytes and iPS differenciated into iHeps	3D encapsulated in PEG-DA hydrogel	Omeprazol Rifampin	Albumin production, Viability, CYP450 expression	Maintenance of a stable hepatic function for hepatocytes encapsulated in hydrogel droplets Perfusion successfully maintained the albumin secretion for 28 days	206

	Fibroblasts: 3T3-J2 murine fibroblasts				The use of IPS cells promote the potential of using the model for patient-specific drug screening	
	HepaRG cell line Co-cultured with HUVEC	3D spheroids using wells inside the biochip	Methotrexate Cis-Diamineplatinum (II) dichloride Acetaminophen Cyclosporin Mitomycin C	Viability, expression of the phase I metabolic enzyme CYP450, albumin and urea secretion	The integration of endotheliocytes with hepatocytes improved hepatic functions Albumin, urea, CYP450 and polarity are better expressed in the liver-on-chip model than those in static condition Demonstration of the toxicity of clinical drugs and heavy metal ions with higher sensitivity than traditional static 3D or 2D culture	207
Environmental toxicity	Primary rat hepatocytes	2D (patterned biochip)	Dichlorodiphenyl-trichloroethane (DDT) Permethrin (PMT)	Viability, albumin and urea secretion, glucose consumption, ROS quantification, omics analysis	Used omics-on-chip approach to study the toxicity of pesticide The combination of different low doses of pesticides induce oxidative stress and cell death Pesticides at high doses provoke hepatotoxicity, perturbation of lipid metabolism and steatose	191 195 196
	HepG2 cell line	3D spheroids using wells inside the biochip	Rotenone (R8875)	Viability, real-Time oxygen Measurement, bile canaliculi activity, mitochondrial activity, glucose consumption, lactate production, ATP/ADP ratio	Cells maintained for 28 days of culture Model capable of monitor real-time changes of metabolic pathways The metabolic shifts demonstrated the toxicity Of Retenone at concentrations considered safe previously	199
	Primary rat hepatocytes	2D (fibronectin coated biochip)	Superparamagnetic iron oxide nanoparticles (SPION)	Viability, albumin and urea synthesis	Maintenance of hepatocytes functions for up to 1 week The biochip is more sensible to the deleterious effect of SPION than static condition Results consistent with the responses of perfused hepatocytes to xenobiotics compared with static models	208

	Primary human hepatocytes	3D spheroids (concave agarose chip)	Copper sulfide nanoparticles (CuSNP)	Viability, albumin and urea secretion, glycogen deposition, mitochondrial membrane potential, ROS	Successfully obtained spheroid in the agarose chip Hepatotoxic effect of CuSNP observed in the biochip Association of the mechanism with the hepatotoxicity	203
	Primary human hepatocytes human primary LSECs Kupffer cells	2D using extracellular matrix sandwich	Ethanol	Viability, albumin secretion, cholesterol production, glycogen storage, cytokine, metabolomic analysis	The Liver chip detected the early critical events of ALD Modelling of the circulating endotoxins Modelling of the injury recover after abstinence from alcohol	209
	primary rat hepatocytes Hepatic stellate cells	3D spheroids (concave microwells)	Ethanol	Viability, albumin and urea secretion	Viability of spheroids is sensible to the ethanol flow rate Development of a fibrosis structure in the exposed model to ethanol Model suitable to study reversible and irreversible alcohol liver disease	204

ALT: alanine aminotransferase, AST: aspartate aminotransferase, GDH: glutamate dehydrogenase ATP: adenosine triphosphate, ADP: adenosine diphosphate, A1AT: alpha-1-Antitrypsin, ROS: reactive oxygen species, GelMa :gGelatin methacryloyl, PET-PAA-AHG: Polyethylene terephthalate - polyacrylic acid - 1-O-(6′-aminohexyl)-D-galactopyranoside, PEG-AHG: poly(ethylene glycol) - 1-O-(6′-aminohexyl)-D-galactopyranoside

Table 2. Examples of multiorgan-on-chip platforms integrating liver used for drug and chemical toxicity studies.

Culture model	Cell organizations/configuration	Drugs / Toxicans	Assays	Outcomes	Ref
Liver: HepG2 cell line Kidney: Hek293 cell line	2D monolayer (collagen coating)	Aflatoxin B1 (AFB1) Benzo-alpha-pyrene (BαP) Rifampicin	Viability, cytotoxicity, albumin and urea secretion, CYPs expression	Efficient toxins and drugs metabolization Multi-faceted physiological phenomena modelling	210
Liver: HepaRG and Human primary hepatic stellate cells (HHSTeC) Intestine: Caco-2 and HT-29 cell lines	Intestine barrier using permeable membrane Liver spheroids using Hanging Drop Plates	Acetaminophen	Viability, Na-K-ATPase, MDR1, GSTA2, CYP3A4 and UGT1A1 expression, APAP uptake, albumin secretion	Maintenance of co-cultured spheroids Formation of a functional intestine barrier cell Low cytotoxicity on the intestine barrier cell even after 24h of treatment	211
Liver: HepG2 cell line Intestine: Caco-2/HT29-MTX cell lines	Intestine barrier using permeable membrane 2D liver monolayer on poly-D-lysine and fibronectin coated surface	Carboxylated polystyrene nanoparticles	Viability, enzyme activity of ALT, AST, GDH and GGT, pH variation	Model demonstrated that nanoparticles traversed the intestinal barrier and reached the liver compartment The interaction between the two organs increased the toxic effect of nanoparticles Model suitable for assessing toxicities of environmental toxicants	212
Liver: HepaRG cell line Lung: NHBE cell line	Human 3D bronchial epithelial barrier Liver spheroids using ultra-low adhesion well plate	Aflatoxin B1 (AFB1)	Permeability, albumin and lactate production, glucose consumption, ATP, CYP1A1/1B1 expression of phase 1 metabolism associated genes	Maintenance of cell functions and viability during 28 days Suitable for testing drug efficacy and safety	213

Liver: HepaRG cell line and HHSteC Lung: bronchial MucilAir culture	Spheroids using ultra-low-attachment microplate MUCILAIR™ for the branchial barrier	Aflatoxin B1 (AFB1)	Viability, barrier permeability albumin production, ATP content, tdT-mediated dUTP-digoxigenin nick-end labelling (TUNEL)/Ki67 staining, LDH release, ATP	Culture for 14 days with maintenance of cells functionalities and viability Organs interactions demonstrated using the toxicity of aflatoxin B1 Model suitable to evaluate the toxicity of inhaled substances	214
Liver: HepG2 (human) and H4IIE (rat) cell lines Lung: L2 lung type II epithelial cells	2D monolayer: cells cultivated on matrigel	Naphthalene	CYP450 1A activity, MTS assay, naphthalene metabolites toxicity, intracellular GSH, hydrogen peroxide (H_2O_2) production	Mode suitable to study the ADME of naphthalene Naphthalene reactive metabolites are produced by the liver but the lung is more sensitive for their effect	215
Liver: HepaRG cell line and HHSteC Neural system: NTera-2/cl.D1 (NT2) cell line	hanging drop for liver spheroids Spinner vessel for neurospheres	2,5-hexanedione	Viability, glucose consumption, lactate and LDH production, gene expression	Maintenance of cell functions and viability during 14 days Correlation between drug toxicity and tissue-tissue communication	217
Liver: HepG2 cell line BBB barrier: primary BMECS and cerebral astrocytes Brain: U87 cell line	2D monolayer: cells cultivated on collagen coating	Paclitaxel (PTX) Capecitabine (CAP) Temozolomide (TMZ)	Barrier permeability, viability, drug metabolites detection by mass spectrometry, TEER measurement	Design of an efficient multi interfaces device Evaluation of anti-brain tumor drugs Correlation between drug response and properties	218
Liver: HepG2 cell line Heart: H9c2 cell line	3D using PepGel™ PGmatrix-Spheroid	Doxorubicin (DOX)	Viability, urea production DOX metabolism	Device allowing to evaluate both parent drug and its metabolites Toxicity of metabolites produced by liver on heart cells	219

Heart: iPSc derived cardiomyocytes Liver: Cryopreserved human primary hepatocytes (PHH)	2D using fibronectin (iPSc) and collagen (PHH) coating	Diclofenac sodium Ketoconazole Hydrocortisone Acetaminophen	Viability, albumin and LDH production, CYP expression Cardiac function	Model suitable for acute and chronic drug exposure associated with transdermal drug delivery	220
Liver: HepG2 and HepaRG cell line Kidney: MDCK cell line	2D using a fibronectin coating	Ifosfamide chloroacetaldehyde	Proliferation, cell cycle repartition, CYP expression	Organs interactions observed through the toxicity of the ifosfamide and its nephrotoxic metabolite produced by the liver The nephrotoxicity of ifosfamide is only observed when associated with its metabolite the chloroacetaldehyde The chloroacetaldehyde decrease viability and causes perturbations of the intracellular calcium release	221

LDH: lactate dehydrogenase, ALT: alanine aminotransferase, AST: aspartate aminotransferase, GDH: glutamate dehydrogenase, GGT: gamma-glutamyl transpeptidase, TEER: transepithelial electrical resistance, ATP: adenosine triphosphate